



Z boson production in Pb+Pb collisions at $\sqrt{s_{NN}} = 5.02$ TeV measured by the ATLAS experiment

The ATLAS Collaboration *

ARTICLE INFO

Article history:

Received 30 October 2019

Received in revised form 27 December 2019

Accepted 27 January 2020

Available online 31 January 2020

Editor: D.F. Geesaman

ABSTRACT

The production yield of Z bosons is measured in the electron and muon decay channels in Pb+Pb collisions at $\sqrt{s_{NN}} = 5.02$ TeV with the ATLAS detector. Data from the 2015 LHC run corresponding to an integrated luminosity of 0.49 nb^{-1} are used for the analysis. The Z boson yield, normalised by the total number of minimum-bias events and the mean nuclear thickness function, is measured as a function of dilepton rapidity and event centrality. The measurements in Pb+Pb collisions are compared with similar measurements made in proton–proton collisions at the same centre-of-mass energy. The nuclear modification factor is found to be consistent with unity for all centrality intervals. The results are compared with theoretical predictions obtained at next-to-leading order using nucleon and nuclear parton distribution functions. The normalised Z boson yields in Pb+Pb collisions lie $1\text{--}3\sigma$ above the predictions. The nuclear modification factor measured as a function of rapidity agrees with unity and is consistent with a next-to-leading-order QCD calculation including the isospin effect.

© 2020 The Author(s). Published by Elsevier B.V. This is an open access article under the CC BY license (<http://creativecommons.org/licenses/by/4.0/>). Funded by SCOAP³.

1. Introduction

The measurement of electroweak (EW) boson production is a key part of the heavy-ion (HI) physics programme at the Large Hadron Collider (LHC). Isolated photons and heavy vector bosons, Z and W, are powerful tools to probe the initial stages of HI collisions. After being created at the initial stage of the collision in high-momentum exchange processes, Z and W bosons decay much faster than the timescale of the medium's evolution. Their leptonic decay products are generally understood to not be affected by the strong interaction; hence they carry information about the initial stage of the collision and the partonic structure of the nuclei.

Measurements performed by the ATLAS and CMS experiments with Z and W bosons decaying leptonically show that production rates of these non-strongly interacting particles are proportional to the amount of nuclear overlap, quantified by the mean nuclear thickness function, $\langle T_{AA} \rangle$ [1–6]. Results obtained with isolated high-energy photons [7,8] are also consistent with this observation.

The transverse momentum and rapidity distribution of Z bosons and the pseudorapidity distribution of muons originating from W bosons measured in Pb+Pb collisions at $\sqrt{s_{NN}} = 2.76$ TeV have been found to be generally consistent with perturbative quantum chromodynamics (pQCD) calculations of nucleon–nucleon

collisions scaled by $\langle T_{AA} \rangle$. Production of Z bosons in Pb+Pb collisions was found to be consistent with next-to-leading-order (NLO) pQCD calculations that do not include nuclear modifications in the treatment of parton distribution functions (PDFs). However, some nuclear modification of PDFs could not be excluded within the precision of the existing Pb+Pb measurements [1,2,7]. The recent ALICE result at $\sqrt{s_{NN}} = 5.02$ TeV shows better agreement with nPDF calculations at forward rapidities [9].

On the other hand, the study of asymmetric p+Pb collisions at $\sqrt{s_{NN}} = 5.02$ TeV shows that including nuclear modifications of PDFs gives a substantially better description of the data than using a free proton PDF. This is seen by comparing the Z boson cross section in p+Pb collisions with pQCD calculations [10–13] and recently also the W boson cross section at $\sqrt{s_{NN}} = 5.02$ TeV and $\sqrt{s_{NN}} = 8.16$ TeV [13,14]. In addition, studies of Z bosons differentially in p+Pb centrality demonstrate that they are a sensitive test of the Glauber model description of nuclear geometry [11].

This letter presents results on Z boson production yield measurement in the $Z \rightarrow \mu\mu$ and $Z \rightarrow ee$ decay channels in Pb+Pb collisions at $\sqrt{s_{NN}} = 5.02$ TeV with the ATLAS detector at the LHC. The data sample was collected in November 2015 and corresponds to an integrated luminosity of 0.49 nb^{-1} . The observables under study are the yield of produced Z bosons in the fiducial kinematic region defined by detector acceptance and lepton kinematics normalised to the number of minimum-bias events, measured differentially in rapidity and event centrality. The Pb+Pb data are compared with pQCD calculations, and the nuclear modification

* E-mail address: atlas.publications@cern.ch.

factor is measured relative to pp cross section previously measured by the ATLAS experiment [15].

2. ATLAS detector

The ATLAS detector [16] covers nearly the entire solid angle¹ around the collision point. It consists of an inner tracking detector surrounded by a thin superconducting solenoid, electromagnetic and hadronic calorimeters, and a muon spectrometer incorporating three large superconducting toroid magnets.

The inner-detector system is immersed in a 2 T axial magnetic field and provides charged-particle tracking in the range $|\eta| < 2.5$. The high-granularity silicon pixel detector covers the vertex region and typically provides four measurements per track, the first hit being in the insertable B-layer [17,18] in operation since 2015. It is followed by the silicon microstrip tracker, which usually provides eight measurements per track. These silicon detectors are complemented by the transition-radiation tracker, which enables radially extended track reconstruction up to $|\eta| = 2.0$.

The calorimeter system covers the pseudorapidity range $|\eta| < 4.9$. Within the region $|\eta| < 3.2$, electromagnetic (EM) calorimetry is provided by barrel and endcap high-granularity liquid-argon (LAr) sampling calorimeters, with an additional thin LAr presampler covering $|\eta| < 1.8$, to correct for energy loss in material upstream of the calorimeters. Hadronic calorimetry is provided by the scintillator-tile calorimeter, segmented into three barrel structures within $|\eta| < 1.7$, and two LAr hadronic endcap calorimeters. The forward calorimeter (FCal) is a LAr sampling calorimeter located on either side of the interaction point. It covers $3.1 < |\eta| < 4.9$ and each half is composed of one EM and two hadronic sections. The FCal is used to characterise the centrality of Pb+Pb collisions as described below. Finally, zero-degree calorimeters (ZDC) are situated at large pseudorapidity, $|\eta| > 8.3$, and are primarily sensitive to spectator neutrons.

The muon spectrometer comprises separate trigger and high-precision tracking chambers measuring the deflection of muons in a magnetic field generated by superconducting air-core toroids. The precision chamber system covers the region $|\eta| < 2.7$ with three layers of monitored drift tubes, complemented by cathode-strip chambers in the forward region, where the background is highest. The muon trigger system covers the range $|\eta| < 2.4$ with resistive-plate chambers in the barrel, and thin-gap chambers in the endcap regions.

A two-level trigger system is used to select events of interest for recording [19]. The level-1 (L1) trigger is implemented in hardware and uses a subset of the detector information to reduce the event rate. The subsequent, software-based high-level trigger (HLT) selects events for recording. Both the electron and muon event selection used in this analysis combine L1 and HLT decision algorithms.

3. Data sets and event selection

All of the analysed data were recorded in periods with stable beam, detector, and trigger operations. Candidate events are required to have at least one primary vertex reconstructed from the inner-detector tracks. In addition, a trigger selection is applied, requiring a muon or an electron candidate above a p_T threshold of

8 GeV or 15 GeV, respectively. The electron-trigger candidate is further required to satisfy a set of loose criteria for the electromagnetic shower shapes [20]. The trigger algorithm implements an event-by-event estimation and subtraction of the underlying-event contribution to the transverse energy deposited in each calorimeter cell [21]. For both the electron and muon candidates, further requirements are applied to suppress electromagnetic background contributions, as described in Section 4.2.

Muon candidates reconstructed offline must satisfy $p_T > 20$ GeV and $|\eta| < 2.5$ and pass the requirements of ‘medium’ identification optimised for 2015 analysis conditions [22]. Offline selected electron candidates are required to have $p_T > 20$ GeV and $|\eta| < 2.47$, although candidates within the transition region between barrel and endcap calorimeters ($1.37 < |\eta| < 1.52$) are rejected. In addition, likelihood-based identification is applied, developed for the Pb+Pb data conditions and based on a general strategy described in Ref. [23].

Events with a Z boson candidate are selected by requiring exactly two opposite-charge muons or electrons, at least one of which is matched to a lepton selected at trigger level. The dilepton invariant mass must satisfy the requirement $66 < m_{\ell\ell} < 116$ GeV consistent with previous ATLAS measurements. A total of 5347 Z boson candidates are found in the muon channel and 4047 in the electron channel.

In order to estimate the geometric characteristics of HI collisions, it is common to classify the events according to the amount of nuclear overlap in the collision. The quantity used to estimate the collision geometry is called the ‘collision centrality’. The centrality determination is based on the total transverse energy measured by both FCal detectors in each event, ΣE_T^{FCal} . This quantity is then mapped to geometric quantities, such as the average number of participating nucleons, $\langle N_{\text{part}} \rangle$, and the mean nuclear thickness function, $\langle T_{\text{AA}} \rangle$, which quantifies the amount of nuclear overlap in a centrality class and is evaluated using a Glauber calculation [24, 25]. The mapping is based on specific studies of an event sample without additional Pb+Pb collisions within the same or neighbouring bunch crossings (pile-up) collected with minimum-bias (MB) triggers. A special treatment is employed for events in the 20% most peripheral interval, where diffractive and photonuclear processes contribute significantly to the MB event sample. This requires extrapolating from the total number of MB events in this region and employing a special requirement on the Z boson event topology, as described in Section 4.2. Table 1 summarises the relationship between centrality, $\langle N_{\text{part}} \rangle$, and $\langle T_{\text{AA}} \rangle$ as calculated with Glauber MC v2.4 [6,26], which incorporates nuclear densities averaged over protons and neutrons. The total number of MB events in the 0–80% centrality interval is $(2.99 \pm 0.04) \times 10^9$, which is then distributed in different centrality intervals according to their size. The quoted uncertainty on the number of MB events includes variations on the ΣE_T^{FCal} value corresponding to the 0–80% centrality interval estimated with the Glauber model. This sample is obtained by selecting events passing MB triggers and excluding the events with a pile-up contribution, where the total sampled integrated luminosity corresponds to the signal selection [25].

Simulated samples of Monte Carlo (MC) events are used to evaluate the selection efficiency for signal events and the contribution of several background processes to the analysed data set. All of the samples were produced with the GEANT4-based simulation [27,28] of the ATLAS detector. Dedicated efficiency and calibration studies with data are used to derive correction factors to account for residual differences between experiment and simulation.

The processes of interest containing Z bosons were generated with the POWHEG-Box v1 MC program [29–32] interfaced to the PYTHIA 8.186 parton shower model [33]. The CT10 PDF set [34] was used in the matrix element, while the CTEQ6L1 PDF set [35]

¹ ATLAS uses a right-handed coordinate system with its origin at the nominal interaction point (IP) in the centre of the detector and the z-axis along the beam pipe. The x-axis points from the IP to the centre of the LHC ring, and the y-axis points upwards. Cylindrical coordinates (r, ϕ) are used in the transverse plane, ϕ being the azimuthal angle around the z-axis. The pseudorapidity is defined in terms of the polar angle θ as $\eta = -\ln \tan(\theta/2)$.

Table 1

Centrality intervals and their corresponding geometric quantities with systematic uncertainties, from Ref. [6,26].

| Centrality [%] | $\langle N_{\text{part}} \rangle$ | $\langle T_{\text{AA}} \rangle [\text{mb}^{-1}]$ | Centrality [%] | $\langle N_{\text{part}} \rangle$ | $\langle T_{\text{AA}} \rangle [\text{mb}^{-1}]$ |
|----------------|-----------------------------------|--|----------------|-----------------------------------|--|
| 0–2% | 399.0 ± 1.6 | 28.30 ± 0.25 | 20–25% | 205.6 ± 2.9 | 9.77 ± 0.18 |
| 2–4% | 380.2 ± 2.0 | 25.47 ± 0.21 | 25–30% | 172.8 ± 2.8 | 7.50 ± 0.17 |
| 4–6% | 358.9 ± 2.4 | 23.07 ± 0.21 | 30–40% | 131.4 ± 2.6 | 4.95 ± 0.15 |
| 6–8% | 338.1 ± 2.7 | 20.93 ± 0.20 | 40–50% | 87.0 ± 2.4 | 2.63 ± 0.11 |
| 8–10% | 317.8 ± 2.9 | 18.99 ± 0.19 | 50–60% | 53.9 ± 2.0 | 1.28 ± 0.07 |
| 10–15% | 285.2 ± 2.9 | 16.08 ± 0.18 | 60–80% | 23.0 ± 1.3 | 0.39 ± 0.03 |
| 15–20% | 242.9 ± 2.9 | 12.59 ± 0.17 | 80–100% | 4.80 ± 0.36 | 0.052 ± 0.006 |
| | | | 0–100% | 114.0 ± 1.1 | 5.61 ± 0.06 |

was used with the AZNLO [36] set of generator-parameter values (tune) for the modelling of non-perturbative effects in the initial-state parton shower. The PHOTOS++ v3.52 program [37] was used for final-state photon radiation in EW processes.

A sample of top-quark pair ($t\bar{t}$) production was generated with the POWHEG-Box v2 generator, which uses NLO matrix-element calculations [38] together with the CT10f4 PDF set [39]. The parton shower, fragmentation and underlying event in nucleon–nucleon collisions were simulated using PYTHIA 6.428 [40] with the CTEQ6L1 PDF set and the corresponding Perugia 2012 tune (P2012) [41]. The top-quark mass was set to 172.5 GeV. The EvtGen v1.2.0 program [42] was used to model bottom and charm hadron decays for all versions of PYTHIA. The total Z boson and top-quark yields in MC samples are normalised using the results of NLO QCD calculations.

The signal MC samples were produced with different nucleon–nucleon combinations (pp , pn , nn) weighted to reflect the isospin composition of lead nuclei. For lead, $A = 208$ and $Z = 82$, so all samples with two neutrons have a weight of $([A - Z]/Z)^2 = 36.7\%$, events with two protons have a weight of 15.5% and the unlike nucleon combinations (pn , np) each have weights of 23.9%.

Once produced, the simulated events were overlaid with MB events taken during the Pb+Pb run. The overlay of data events was done such that the MC simulation accurately reflects detector occupancy conditions present in the Pb+Pb run. The MB events used for the overlay were sampled such that the centrality distribution, based on the total transverse energy deposited in the forward calorimeters, approximates that of Z boson events, which are generally biased to more-central collisions. The simulated events were finally reconstructed by the standard ATLAS reconstruction software.

4. Analysis

4.1. Measurement procedure

The differential Z boson production yield per MB event is measured within a fiducial phase space defined by $p_T^e > 20$ GeV, $|\eta_e| < 2.5$ and $66 < m_{\ell\ell} < 116$ GeV. The yields in both the electron and muon channel are calculated using

$$N_Z^{\text{fid}} = \frac{N_Z - B_Z}{\epsilon_{\text{trig}}^Z \cdot C_Z}, \quad (1)$$

where N_Z and B_Z are the number of selected events in data and the expected number of background events, respectively, and ϵ_{trig}^Z is the trigger efficiency per Z boson candidate measured in data and described in Section 4.3.

A correction for the reconstruction efficiency, momentum resolution and the final-state radiation effects is applied with the bin-by-bin correction factor C_Z which is obtained from MC simulation as

$$C_Z = \frac{N_Z^{\text{MC,sel}}}{N_Z^{\text{MC,fid}}}.$$

Here, $N_Z^{\text{MC,sel}}$ is the number of events passing the signal selection at the detector level. The number of selected events is corrected for measured differences between data and simulation in lepton reconstruction and identification efficiencies. The denominator $N_Z^{\text{MC,fid}}$ is computed by applying the fiducial phase-space requirements to the generator-level leptons originating from Z boson decays. The measurement is corrected for QED final-state radiation effects by using the generator-level lepton kinematics before photon radiation.

The value of C_Z in the fiducial acceptance averaged over all centralities is determined from MC simulation after reweighting as explained in Section 3. It is 0.659 and 0.507 in the $Z \rightarrow \mu^+\mu^-$ and $Z \rightarrow e^+e^-$ decay channels, respectively. The uncertainty due to the size of the simulated sample is at the level of 0.1% for each decay channel and is not the dominant uncertainty.

The rapidity, momentum and centrality dependence of C_Z is calculated from the simulation as

$$C_Z(p_T, y, \Sigma E_T^{\text{FCal}}) = F(p_T, y)G(y, \Sigma E_T^{\text{FCal}}), \quad (2)$$

where $F(p_T, y)$ is the centrality-averaged efficiency calculated per y and p_T interval of the dilepton system and $G(y, \Sigma E_T^{\text{FCal}})$ is a parabolic parameterisation of a correction factor accounting for the centrality and rapidity dependences of the efficiency. In each rapidity bin, the factor G is obtained from a fit of the ratio of the efficiency in a particular centrality bin to the value averaged over all possible centrality values.

Nuclear modification is quantified by measuring the ratio of the Z boson production rate, scaled by the mean nuclear thickness function, to the Z boson production cross section in pp collisions, a quantity known as the nuclear modification factor:

$$R_{\text{AA}}(y) = \frac{1}{\langle T_{\text{AA}} \rangle N_{\text{evt}}} \frac{dN_{\text{Pb+Pb}}^Z/dy}{d\sigma_{pp}^Z/dy},$$

where $\langle T_{\text{AA}} \rangle$ is the nuclear thickness function in a given centrality class, $(1/N_{\text{evt}})dN_{\text{Pb+Pb}}^Z/dy$ is the differential yield of Z bosons per inelastic MB event measured in Pb+Pb collisions and $d\sigma_{pp}^Z/dy$ is the differential Z boson cross section measured in pp collisions [15]. A deviation from unity in R_{AA} indicates the nuclear modification of the observable. The value of R_{AA} is expected to be greater than unity by about 2.5%, based on MC simulation, due to the higher Z boson production cross section in proton–neutron and neutron–neutron interactions which are present in Pb+Pb collisions and amount to 84.5% of the total hadronic cross section. This is later referred to as the ‘isospin effect’ and is not accounted for in the definition of R_{AA} .

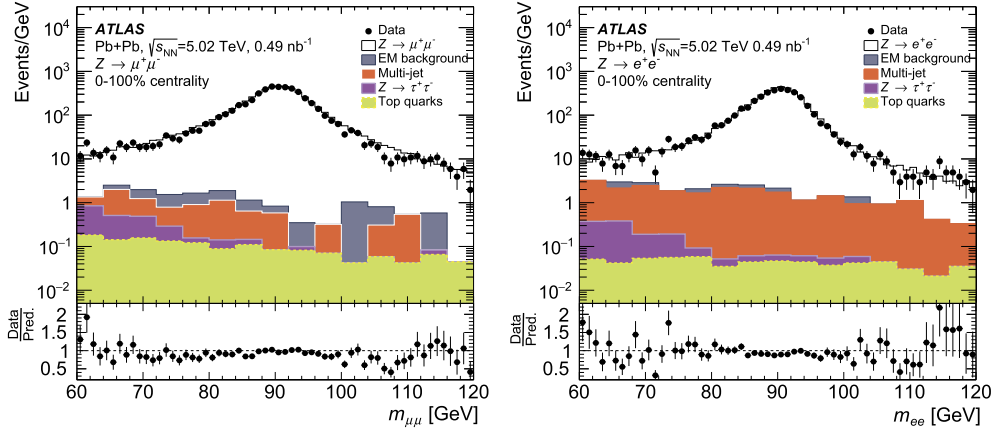


Fig. 1. Centrality-integrated detector-level invariant mass distribution of (left) dimuon and (right) dielectron pairs together with the $Z \rightarrow \tau^+\tau^-$, top quark, multi-jet and EM background contributions. Only the statistical uncertainties of the data are shown.

4.2. Background determination

There are two background source categories studied in this analysis. The first includes the same background sources that are studied in pp collisions [15] and the second includes additional background sources specific to the Pb+Pb collision system.

Background contributions in the first category are expected from $Z \rightarrow \tau^+\tau^-$, top-quark pair production and multi-jet events. The first two contributions are evaluated from dedicated simulation samples, whereas the multi-jet background contribution is derived using a data-driven approach. The $Z \rightarrow \tau^+\tau^-$ background is found to be 0.05% of all signal candidates in the muon channel and 0.06% in the electron channel. The top-quark background amounts to 0.08% in the muon channel and 0.05% in the electron channel. The background contribution from W boson decays and W +jet production is found to be negligible.

The multi-jet background originates from jets, misidentified hadrons and, in the electron channel, from converted photons. In the muon channel, its contribution is estimated from the distribution of the same-sign Z boson candidates in rapidity and centrality. Due to the low charge misidentification rate in the muon spectrometer, their invariant mass distribution does not exhibit a peak in the Z boson mass region. In the muon channel this background amounts to 0.5% of all signal candidates. In the electron channel, there is a significant contribution from charge misidentification, fakes and conversions. The electron same-sign pairs therefore cannot be used to estimate the multi-jet background. This contribution to the selected event sample in the electron channel is estimated using a background template obtained from the data in Z boson rapidity and event centrality. The template is derived from a subset of the signal sample that corresponds to electrons from jets, i.e. electrons with a very poor reconstruction quality [23] that also satisfy $p_{T\text{cone}20}/2p_T > 0.05\Sigma E_T^{\text{FCal}} + 0.025$, where $p_{T\text{cone}20}$ is the total transverse momentum measured inside the cone of size $R = 0.2$ around the electron track. The template is normalised to the number of same-sign data candidates in the low-mass region of $60 < m_{ee} < 70$ GeV after the signal MC subtraction. Due to the small number of signal candidates satisfying this condition, same-sign electron pairs with the same kinematic requirements are also added to this background template. The shape of the obtained multijet template is shown in Fig. 1. This background amounts to 2% of all signal candidates in the electron channel.

The background contributions specific to Pb+Pb come from two main sources. The first is due to pile-up when more than a single Pb+Pb collision is recorded simultaneously or in a nearby bunch crossing. The second is the production of additional Z boson can-

didates by photon-induced reactions produced by the intense electromagnetic fields generated by the colliding ions (below referred to as ‘electromagnetic background’). Pile-up distorts the transverse energy measured in the FCal and causes reconstructed Z bosons to be assigned to an incorrect centrality interval. Pile-up events from other collisions in the same bunch crossing (in-time pile-up) increase the ΣE_T^{FCal} , shifting the Z boson candidate to a more-central interval. Alternatively, if a pile-up collision precedes the trigger event (out-of-time pile-up), its contribution to the ΣE_T^{FCal} can be negative, due to the time response of the electronic signal shapers used in the calorimeters [43]. In this case, the Z boson candidate is shifted to a more-peripheral interval. Both processes depend on the instantaneous luminosity during data taking. At any time during the HI run the number of hadronic interactions per bunch crossing was less than 0.01. To preserve the accuracy of the total yield measurement, no pile-up removal procedure was applied to the selected events. However, due to the fact that the Z boson production scales linearly with $\langle T_{AA} \rangle$ [1], the increase in the FCal transverse energy in in-time pile-up events transfers candidates from less populated to more-populated centrality intervals, thus having a very small effect and changing the average number of counts in the most central collisions by an insignificant amount. Contrary to that, the reduction in the ΣE_T^{FCal} transfers out-of-time pile-up events from more-populated to less-populated centrality intervals, thus making a larger relative contribution to the more-peripheral events. The effect has been studied using several independent data-driven and simulation-based approaches. The largest contribution to the most peripheral 80–100% centrality interval due to this type of the pile-up is less than 2%, i.e. less than one count, and is significantly less in any other centrality range.

A non-negligible relative contribution to the dileptons in the Z boson mass range in peripheral centrality intervals is expected from electromagnetic background sources. On the other hand, the expected rate of signal events in those peripheral centrality bins is low. Two photon-induced processes are expected to contribute to the background: photon-photon scattering, $\gamma\gamma \rightarrow \ell^+\ell^-$ [44–46] and photon-nucleus scattering $\gamma + A \rightarrow Z \rightarrow \ell^+\ell^-$ [47]. Although measurements of exclusive high-mass dilepton production have been performed in pp and Pb+Pb collisions by ATLAS [48] and in pp collisions by CMS [49] a photo-nuclear Z boson production has not yet been observed in HI collisions. When the impact parameter of the photon-induced processes is larger than twice the nuclear radius such processes are referred to as ultra-peripheral collisions, and in these they are not obscured by hadronic interactions. Both physics processes are characterised by large rapidity gaps on one or both sides of the detector (regions with no particle production

recorded in the detector), which are used in this analysis to measure and subtract these backgrounds. The rapidity gap estimation is implemented using a similar technique as developed in Ref. [50].

In the 50–100% (peripheral) centrality intervals, there is an additional requirement of a ZDC signal coincidence in order to suppress the electromagnetic background contributions. The energy measured in either detector is required to be at least 1 TeV, corresponding to 40% of the energy deposition of a single neutron. Without using any ZDC coincidence requirement in the event selection, 34 events with a rapidity gap greater than 2.5 units are found in the two decay channels. Since the estimated number of hadronic Z boson candidates with such a gap is below 0.05, all of these events are considered to be produced by photon-induced reactions and are removed from the sample. Events without gaps can have a photon-induced dilepton pair as well, if the rapidity gap is filled by particles originating from a simultaneous nucleon–nucleon interaction. These events would appear in the centrality intervals defined by the ΣE_T^{FCal} deposition from the hadronic interaction.

Following Ref. [51], photon-induced reactions occurring simultaneously with hadronic collisions can be identified using both the angular and momentum correlations of final-state dilepton pairs. One variable used to quantify these correlations is the dilepton acoplanarity, defined as $\alpha \equiv 1 - |\phi^+ - \phi^-|/\pi$, where ϕ^\pm are the azimuthal angles of the two opposite-charge leptons. The same observable is used in this analysis to extract the contribution of photon-induced reactions to the measured Z boson production. Based on the MC signal simulation and measurements in the 0–50% centrality interval, $(13.3 \pm 0.4)\%$ of Z boson candidates produced by hadronic collisions have acoplanarity below 0.01. On the other hand, among the 34 events with a rapidity gap greater than 2.5 units which were rejected from the sample as pure photon-induced events, 26 are found to have $\alpha < 0.01$, corresponding to a fraction of 76%. This demonstrates that the acoplanarity is sensitive to photon-induced reactions in the Z boson invariant-mass region. This allows the photon-induced background to be estimated in all centrality intervals by comparing the number of Z boson candidates in a given centrality interval with the number of candidates with $\alpha < 0.01$.

It is estimated that in the 80–100% centrality interval, besides the events with a large rapidity gap, 7 ± 3 out of 28 remaining candidates originate from photon-induced reactions. In the 60–80% interval this number is 15 ± 5 out of 182, and in the 50–60% interval it is 18 ± 8 out of 258, where the uncertainty includes statistical and systematic uncertainties in the background, but not in the number of event candidates. In more-central collisions, the method of estimating the photon-induced background is limited by the statistical precision of the sample and this contribution is consistent with zero. Rapidity distributions in centrality intervals are normalised to the estimated number of signal events and an additional systematic error is assigned in each interval to account for the EM background subtraction procedure.

Fig. 1 shows the invariant mass distribution of backgrounds from all considered sources for both decay channels integrated in event centrality. The EM background shape shown in Fig. 1 is derived from the events containing large rapidity gaps and is normalised to the total estimated number of background candidates quoted above.

4.3. Detector performance corrections

After subtracting background contributions, the number of Z boson candidates is corrected for the trigger efficiency and detection efficiency, according to Eq. (1). All the correction factors are derived directly from the current data set used in the analysis,

with the exception of the lepton momentum calibration corrections that are derived from pp collision data, and extrapolated to the Pb+Pb dataset conditions. The trigger efficiency per reconstructed Z candidate ϵ_{trig}^Z is derived from the efficiency of the single-lepton trigger ϵ_ℓ via the relation $\epsilon_{\text{trig}}^Z = 1 - (1 - \epsilon_{\ell_1})(1 - \epsilon_{\ell_2})$, where the indices refer to the two leptons forming the candidate pair. In order to obtain ϵ_{trig}^Z as a function of the dilepton p_T and y which is further applied as a correction per dilepton candidate, kinematic distributions of the decay products are taken from MC simulation.

Muon and electron trigger efficiencies are measured using a tag-and-probe method [19,22,23] as a function of η and ϕ . The tag lepton is required to be reconstructed with high quality and very low probability of background contamination and to be matched to a lepton selected at trigger level. The probe lepton, satisfying the analysis reconstruction and identification requirements, is paired to it to give an invariant mass in the range $66 < m_{\ell\ell} < 116$ GeV. The background contribution to this measurement is estimated from the number of same-sign pairs and amounts to 0.8% and 3.5% in the muon and electron channels, respectively.

The single-muon trigger efficiency in the endcap region of the detector ($1.05 < |\eta| < 2.4$) is measured to be around 85%, and in the barrel region ($|\eta| < 1.05$) it varies between 60% and 80%. A significant dependence of the efficiency on the muon azimuthal angle ϕ was measured and thus the trigger efficiency correction is derived as a function of both ϕ and η . The single-electron trigger efficiency is measured to be around 95% in the endcap region of the calorimeter ($1.52 < |\eta| < 2.47$) and it increases slightly to 97% in the barrel ($|\eta| < 1.37$). A significant dependence on the electron p_T was measured, and the efficiency rises from 85% to 97% in the range from 20 to 100 GeV integrated over η . The single-electron trigger efficiency is thus derived as a function of p_T and η . The average ϵ_{trig}^Z is $(94.2 \pm 0.2)\%$ in the muon channel and $(99.74 \pm 0.03)\%$ in the electron channel, constant with the event centrality within 1%.

Selection requirements including the muon reconstruction and identification are imposed on muon candidates used in the analysis. The efficiency of the selection criteria is measured using a tag-and-probe method in $Z \rightarrow \mu^+\mu^-$ events [22] and compared with simulation. Ratios of the efficiencies determined in data and simulation are applied as scale factors (SF) to correct the simulated events. Since the measured efficiencies are found to have negligible dependence on the muon momentum in the selected kinematic region and a very weak centrality dependence, the SF are evaluated only as a function of muon η . The centrality dependence of the SF is taken into account in the evaluation of systematic uncertainties. The combined reconstruction and identification efficiency for medium-quality muons typically exceeds 84% in both the data and simulation with good agreement between the two estimates. The largest difference is observed in the endcap region ($|\eta| > 1.8$). Ultimately, the SF values for three different η regions are as follows: 0.97 ± 0.01 for $|\eta| < 0.8$, 0.99 ± 0.01 for $0.8 < |\eta| < 1.8$ and 1.04 ± 0.02 for $|\eta| > 1.8$.

Electron candidates used for the analysis are required to satisfy selection criteria related to reconstruction and identification. The efficiency of the selection is measured using a tag-and-probe method in $Z \rightarrow e^+e^-$ events, as described in Ref. [23], and compared with simulation to derive electron scale factors. Measurements are performed as a function of the electron η , p_T and event centrality. The electron reconstruction and identification efficiency is measured to be typically 70% in the endcap ($|\eta| > 1.52$) with good agreement between the data and the simulation. The SF is measured to be 1% away from unity with a precision of 3% in that region. In the barrel region ($|\eta| < 1.37$) the efficiency is measured

to be around 80% while in the MC simulation the efficiency reaches 85%. Therefore, in this region a significant SF is applied, measured with a precision of 3–5%.

The lepton momentum scale and resolution corrections are derived using the pp signal MC samples and are applied to the simulation for both the electrons and muons. For the reconstructed muons, these corrections are derived as a function of the muon η and ϕ [22]. The correction factors are chosen such that they minimise the χ^2 between the muon-pair invariant mass distributions in data and simulation. The energy scale of reconstructed electrons is corrected by applying to the data a per-electron correction factor. The momentum scale correction factors are derived from a comparison of the electron-pair invariant mass between simulation and data.

5. Systematic uncertainties

In both channels, the trigger efficiency is derived from the tag-and-probe results in the data. The statistical limitation of the measured sample determines the uncertainty associated with the trigger correction. Although the uncertainties in each bin are relatively large in the muon trigger efficiency, after propagating this uncertainty to the dimuon efficiency, where only one of the muons is required to fire the trigger, the total uncertainty is quite small, between 0.2% and 0.5% when derived as a function of centrality and 0.1–0.2% when derived as a function of Z boson rapidity. The uncertainty is propagated using MC pseudo-experiments and the uncertainties in the linear fit coefficients of the trigger efficiency as a function of centrality. In the electron channel this uncertainty is at most 0.5%.

The NLO cross section of the background samples of $Z \rightarrow \tau^+\tau^-$ and top-quark production is varied by 10% to derive the corresponding uncertainties [15]. However, in both decay channels the multi-jet background dominates the uncertainty contribution. In the muon channel, the multijet background contribution is varied by 10% according to the level of statistical uncertainty in the number of same-sign candidates. This source produces 0.01–0.1% uncertainty in rapidity bins and up to 0.2% uncertainty in centrality bins. In the electron channel, the multi-jet template normalisation is varied by 20%, which corresponds to the level of statistical uncertainty in the number of same-sign candidates in the low-mass control region. The overall contribution to the systematic uncertainty is about 0.5% in rapidity bins and 0.5–2% in centrality bins.

In the 50–100% centrality interval, the uncertainty in subtracting the photon-induced background is evaluated by considering two sources. The first source is the compatibility between the acoplanarity cut efficiencies for hadronic Z boson production evaluated from data and simulation. An uncertainty of 0.4% accounts for this difference. For the second source, the uncertainty in the background rejection efficiency of the acoplanarity cut is evaluated from the candidates with large rapidity gaps. This uncertainty has two contributions. One is the statistical uncertainty of the event sample with large rapidity gaps, which amounts to 7%. The other contribution is due to the observed differences between the acoplanarity distributions for electrons and muons, which amounts to about 8%. In the 0–50% centrality interval, where the background subtraction is not performed, an uncertainty of 0.4%, evaluated from the difference between the data and simulation acoplanarity distributions, is introduced to account for a possible residual EM background contribution.

Uncertainties in the determination of lepton reconstruction and identification efficiency scale factors, as well as the parameterisation of the centrality dependence of the total correction affect the measurements through the correction factors C_Z .

In the muon channel, the scale factors in the three η regions described in Section 4.3 are modified by their errors to derive the corresponding systematic uncertainty of C_Z . In addition, the impact of the measured SF dependence of the final C_Z value on the event centrality is also evaluated. The total relative uncertainty from these two sources ranges from 3.1% at midrapidity ($|\eta| < 0.5$) to 4.5% at forward Z boson rapidities and gives a contribution, constant as a function of the event centrality, of $\sim 3.4\%$ for Z boson yields.

The main contribution to the systematic uncertainty in the electron channel comes from the uncertainties in measuring the reconstruction efficiency scale factor. Uncertainties related to this efficiency are classified as either correlated or uncorrelated, and are propagated accordingly to the final measurement uncertainty. The correlated uncertainty component of the SF is obtained by varying the requirements on the tag electron identification and isolation and on the invariant mass of the tag-and-probe pair. The statistical, uncorrelated, components of the scale factor uncertainties are propagated to the measurements via MC pseudo-experiments, while the systematic components are propagated as a single variation fully correlated across all electron η intervals. This source gives a 2.5–5% uncertainty as a function of rapidity and around 3% for all centrality intervals.

The effect of the calibration and energy scale correction uncertainty of electrons and muons is negligible.

An additional uncertainty of the bin-by-bin correction is due to the parameterisation of the rapidity and centrality dependence of C_Z described in Eq. (2) and it stems primarily from the statistical uncertainty of the MC data set. To estimate uncertainties associated with these assumptions the parameters of the function $G(y, \Sigma E_T^{\text{FCal}})$ are varied by the errors of the parameters of the parabolic fit including covariance between the parameters. The data are corrected with these variations, and the difference between these results and the standard correction are taken as an estimate of the systematic uncertainty. In the muon channel the uncertainty associated with this source ranges from 0.4% to 1.4% in rapidity bins and is constant at $\sim 0.5\%$ as a function of centrality, with the exception of the most peripheral bin where the uncertainty is $\sim 1\%$. In the electron channel, the uncertainty as a function of the rapidity ranges from 0.4% to 1.6% and is $\sim 1\%$ for most centrality intervals, although in the most peripheral bin this contribution rises to $\sim 2\%$.

For both channels and the combined result, the uncertainties of the geometric parameters ($\langle T_{AA} \rangle$ and $\langle N_{\text{part}} \rangle$) listed in Table 1 range from about 1% in central collisions to about 12% in peripheral collisions. These are treated as fully correlated between the channels. Finally, the total uncertainty for the pp measurement [15] used for the R_{AA} calculation is 2.3%.

6. Results

The rapidity distributions of the Z boson yield for the muon and electron decay channels, normalised by the number of MB events and mean nuclear thickness function $\langle T_{AA} \rangle$, are shown in the upper-left panel of Fig. 2. The upper-right panel of the figure shows the $\langle N_{\text{part}} \rangle$ dependence of the normalised Z boson yield in the fiducial acceptance where the systematic uncertainties of the $\langle N_{\text{part}} \rangle$ values are scaled by a factor of three for clarity. The measurements performed in the two channels are combined using the Best Linear Unbiased Estimate (BLUE) method [52], accounting for the correlations of the systematic uncertainties across the channels and measurement bins. The combined result is shown in Fig. 2 together with the combined statistical and systematic uncertainties. The level of agreement between the channels shown in the lower

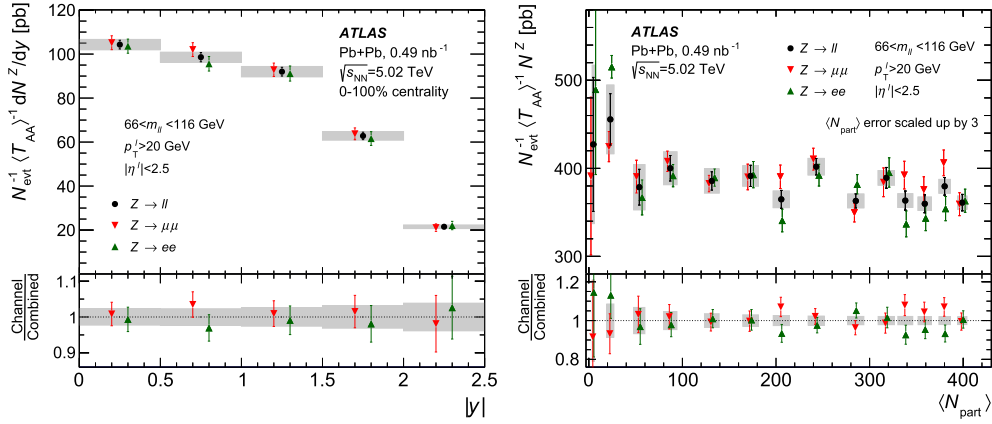


Fig. 2. Normalised Z boson yields measured in the muon and electron decay channels together with the combined yield as a function of (left) rapidity and (right) $\langle N_{\text{part}} \rangle$. Lower panels show the ratio of individual channels to the combined result. The error bars in the upper panels show the total uncertainty for muons and electrons and the statistical uncertainty for the combined data. In the lower panels, the error bars show the statistical uncertainty. The shaded band (left) and boxes (right) show the systematic uncertainty of the combined result in both panels. The width of each error box in the right panel corresponds to the systematic uncertainty of $\langle N_{\text{part}} \rangle$, scaled by a factor of three for clarity. The points corresponding to muon and electron decay channels are shifted horizontally in each panel relative to the bin centre.

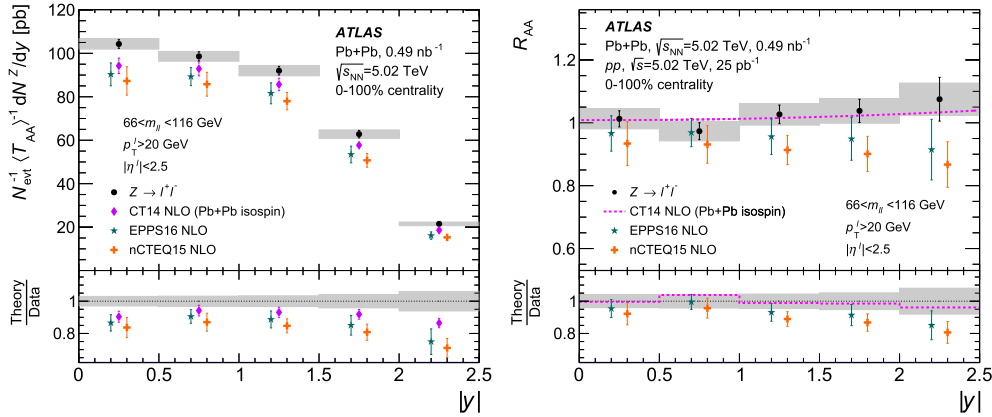


Fig. 3. The upper panels show the rapidity dependence of (left) the normalised Z boson yields and (right) of the R_{AA} compared with theoretical predictions. The lower panels show the ratio of the theoretical predictions to the data. The expected contribution of the isospin effect to the R_{AA} is shown in the upper-right panel by the dashed line. The error bars on the data points indicate the statistical uncertainties and the shaded boxes show the systematic uncertainties. The error bars on predictions show the theoretical uncertainty. The points corresponding to nuclear PDF predictions are shifted horizontally relative to the bin centre for clarity.

panels of the figure is quantified as $\chi^2/N_{\text{dof}} = 1.7/5$ as a function of rapidity and $\chi^2/N_{\text{dof}} = 21.6/14$ as a function of centrality.

The measured Z boson yields are compared with theoretical predictions obtained using a modified version of DYNLO 1.5 [53, 54] optimised for fast computations. The calculation is performed at $O(\alpha_S)$ in QCD and at leading order in the EW theory, with parameters set according to the G_μ scheme [55]. The input parameters (the Fermi constant G_F , the masses and widths of W and Z bosons, and the CKM matrix elements) are taken from Ref. [56]. The DYNLO predictions are calculated using the free proton PDF set CT14 NLO [57] typically used to compare with the pp data and, additionally, the nuclear PDF sets nCTEQ15 NLO [58] and EPPS16 NLO [59], which are averaged over each Pb nucleus. In addition, the parton-level NLO prediction from the MCFM code [60], interfaced to the CT14 NLO PDF set, is calculated. This takes into account the isospin effect, due to different partonic compositions of protons and neutrons in the Pb nuclei, which is neglected in the DYNLO calculations. The renormalisation and factorisation scales, respectively denoted by μ_R and μ_F , are set to the value of lepton pair invariant mass. The uncertainties of these predictions are derived as follows. The effects of PDF uncertainties are evaluated from the variations corresponding to each NLO PDF set. Uncertainties due to the scales are defined by the envelope of the variations obtained by changing μ_R and μ_F by a factor of two from their

nominal values and imposing $0.5 \leq \mu_R/\mu_F \leq 2$. The uncertainty induced by the strong coupling constant is estimated by varying α_S by ± 0.001 around the central value of $\alpha_S(m_Z) = 0.118$, following the prescription of Ref. [57]; the effect of these variations is estimated by comparing the CT14nlo_as_0117 and CT14nlo_as_0119 PDF sets [57] to CT14 NLO. Imperfect knowledge of the proton PDF and the scale variations are the main contributions to the total theory uncertainties. In calculating the R_{AA} predictions, only the nuclear PDF uncertainties contribute since the CT14 NLO uncertainties cancel.

In Fig. 3 the normalised Z boson yield is compared between the combined measurement and the theoretical predictions calculated with the CT14, nCTEQ15 and EPPS16 NLO PDF sets, with uncertainties assigned as previously described. All calculations lie 1–3 σ below the data in all rapidity intervals, integrated over event centrality. Calculations using nuclear PDF sets deviate from the data more strongly than calculations based only on the CT14 NLO PDF set. A similar observation for the CT14 PDF was made in the pp collision system [15] where systematic deviations from the measured values are observed for calculations made at the NNLO. When comparing the measured R_{AA} with calculations, shown in the right panel of Fig. 3, residual deviations from the data are observed. The trend observed in data is consistent with the isospin effect only, expected from the different valence quark content of

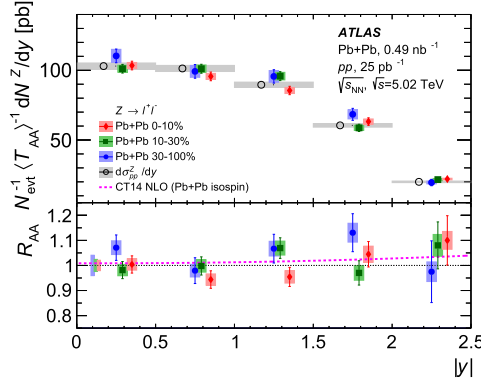


Fig. 4. Normalised Z boson yield versus rapidity measured in three centrality intervals: peripheral 30–100% (blue circles), mid-central 10–30% (green squares) and central 0–10% (red diamonds). The differential Z boson cross sections measured in pp collisions are shown by open circles [15]. The error bars on the data points indicate the statistical uncertainties and the shaded boxes show the total systematic uncertainties. The lower panel shows the R_{AA} and the contribution from the isospin effect calculated with CT14 NLO PDF (dashed line). The shaded boxes at unity indicate the combined uncertainty from the pp data added in quadrature to the T_{AA} uncertainty. The points in each centrality interval are shifted horizontally relative to the bin centre for clarity.

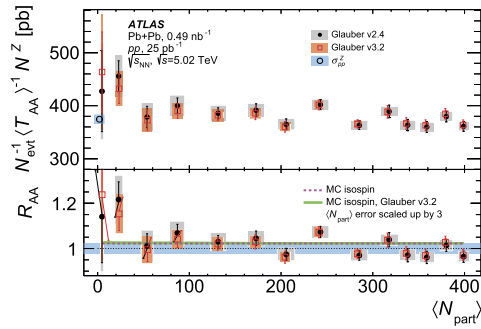


Fig. 5. The upper panel shows the normalised Z boson yield as a function of $\langle N_{part} \rangle$. The integrated fiducial cross section measured in the pp system is shown at $N_{part} = 2$ (open circle). The lower panel shows the nuclear modification factor. The error bars on the data points indicate the statistical uncertainties and the shaded boxes show the total systematic uncertainties. The blue shaded band indicates the total uncertainty of the pp data. The figure shows the results calculated with Glauber MC v2.4 [24] and v3.2 [61]. The dashed and the full line indicate CT14 NLO PDF calculations that account for isospin effects for the two Glauber MC versions. The width of the error box for each centrality interval corresponds to the systematic uncertainty in $\langle N_{part} \rangle$, scaled up by a factor of three for clarity.

protons and neutrons in the Pb nucleus, shown in the upper-right panel of Fig. 3 by the dashed line. These results are in contrast with recent measurements of EW bosons in $p+Pb$ collisions [11, 14] which favour nPDF sets to describe the data.

Fig. 4 shows the normalised Z boson yield as a function of rapidity for three centrality intervals. The results are consistent with each other within their respective statistical uncertainties. The size of the current data sample precludes making a more definitive statement about any possible modification of the Z boson rapidity distribution with centrality.

Fig. 5 shows the centrality dependence of the normalised Z boson yield and of R_{AA} compared with results from pp collisions and Glauber MC. The point corresponding to the pp cross section [15] is shown in the plot at $N_{part} = 2$. The results are derived from Glauber MC v2.4 and a newer version v3.2 following the same procedure as described in Ref. [6]. The results are found to be consistent with each other within experimental uncertainties. The new Glauber MC calculation [61] implements a more advanced treatment of the nuclear density profile and an updated experimental

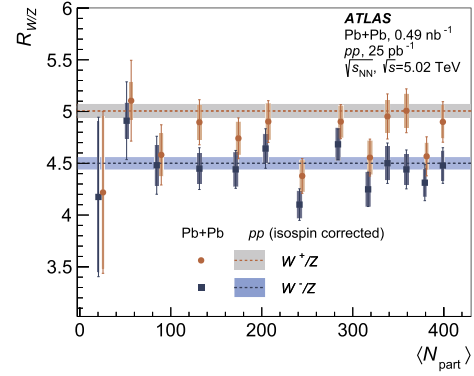


Fig. 6. Ratios of W^+ (circles) and W^- (squares) yields measured in the same data set [6] to the yields of Z bosons versus $\langle N_{part} \rangle$ compared with the ratios measured in pp data [15] (shaded bands) scaled by isospin factors obtained from the CT14 NLO PDF calculation. The error bars on the data points indicate the statistical uncertainties and the shaded boxes show the total systematic uncertainties. The points are shifted horizontally relative to the bin centre for clarity.

value of the nucleon–nucleon inelastic cross section. From these two updates, the former directly affects the normalised Z boson yield derived in this analysis while the updated cross section value has no appreciable effect. The new model also leads to a set of reduced systematic uncertainties compared with the previous version.

In the estimation of the isospin effect contribution shown with dashed and full lines in Fig. 5, the Glauber MC v3.2 model accounts for the slightly larger radius of the neutron distribution compared to the protons in the Pb nucleus, often called the neutron skin effect. However, due to the weak dependence of Z boson production on the isospin content of the colliding baryons, the predictions of the two Glauber MC versions give essentially the same result.

The normalised yields are consistent with the pp cross section at all measured centralities and show only a weak dependence on N_{part} . The values of R_{AA} , shown in the lower panel, are consistent with unity within the total uncertainty. When the isospin effect is taken into account as shown with the dashed line, the model seems to agree better with the data at low N_{part} values rather than at high values. To quantify the dependence of R_{AA} on N_{part} , the data are fit to a linear function. Including statistical and systematic uncertainties the decrease in the R_{AA} value between the most-peripheral (80–100%) and most-central (0–2%) centrality intervals is found to be $(10 \pm 7)\%$ and $(6 \pm 6)\%$ for Glauber MC v2.4 and v3.2, respectively.

The Z boson measurement is used to compare the N_{part} dependence of W [6] and Z boson production by calculating their yield ratios as shown in Fig. 6, where the uncertainties of the two measurements are conservatively treated as uncorrelated. The data points are compared with the ratio measured in pp collisions [15] that is scaled by the isospin factors calculated using the CT14 NLO PDF set. The measurements for both channels are found to be consistent with the scaled pp measurement and show a constant behaviour as a function of centrality.

The trend of the points shown in Fig. 5 for Z bosons is different from the trend observed by the ALICE Collaboration in the measurements with charged hadrons with high transverse momentum [62]. It was recently shown in Ref. [63], that the R_{AA} in peripheral nucleus–nucleus collisions can deviate from unity due to a biased classification of the event geometry for events containing a hard process. In that analysis, the value of R_{AA} without any nuclear effects was determined by using the HG-PYTHIA model [63], which can create an ensemble of events where the HIJING [64] event generator is used to determine the number of hard sub-interactions for each event, and the particle production is determined solely by

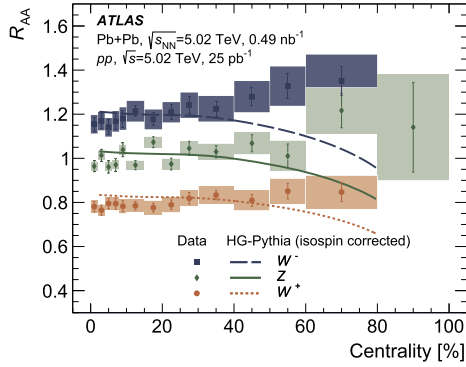


Fig. 7. Nuclear modification factor R_{AA} in centrality intervals compared with the HG-PYTHIA model [63] scaled by the isospin factors obtained from the CT14 NLO PDF calculation. The error bars on the data points indicate the statistical uncertainties and the shaded boxes show the total systematic uncertainties. The model accounts for a biased classification of the event geometry for events containing a hard process. The bins are ordered in centrality percentile, starting from central events on the left towards more peripheral on the right. The Z boson measurement extends to the most peripheral 80–100% centrality interval. The comparison is shown in the 0–80% centrality interval where the different smearing of the ATLAS centrality estimator (ΣE_T^{FCal}) is found to have a negligible effect.

superimposing a corresponding number of PYTHIA 6.4 [40] events. The model is able to qualitatively explain the ALICE measurement in the peripheral region.

Fig. 7 shows the R_{AA} for W^\pm [6] and Z bosons compared with the HG-PYTHIA model. To compare the model with the measurements of massive electroweak bosons the results are corrected for the isospin effect using the CT14 NLO PDF. All three data sets show trends that are consistent between the species, but that differ from their corresponding model predictions. This suggests that the apparent suppression mechanism [63] that explains the ALICE data [62] for the yields of high- p_T charged particles does not have the same effect on the yields of massive electroweak bosons.

7. Summary

The Z boson production yield per minimum-bias collision, scaled by the mean nuclear thickness function $\langle T_{AA} \rangle$ is reported in Pb+Pb collisions at a nucleon–nucleon centre-of-mass energy $\sqrt{s_{NN}} = 5.02$ TeV. The measurement is based on data taken by the ATLAS detector at the LHC corresponding to an integrated luminosity of 0.49 nb^{-1} . Normalised yields are reported in the electron and muon decay channels, differentially in rapidity and collision centrality in the mass window $66 < m_{\ell\ell} < 116$ GeV. The fiducial region is defined using the lepton kinematics and detector acceptance. The electron channel and muon channel results are found to agree within the measurement precision and are combined for the final result.

The normalised Z boson yields measured in Pb+Pb collisions are $1\text{--}3\sigma$ higher than NLO pQCD predictions with both free and nuclear PDF sets, where the difference increases towards forward Z boson rapidity. Calculations using nuclear PDF sets deviate from the data more strongly than calculations based only on the CT14 NLO PDF set which is in contrast with recent EW boson measurements performed in the p+Pb system. The nuclear modification factor is measured differentially as a function of Z boson rapidity and event centrality. It is found to be consistent with unity in centrality and to agree with the prediction based on the CT14 PDF set that takes isospin into account. This behaviour is also consistent with the ATLAS measurement performed with W bosons. The yield ratios W/Z are found to be constant as a function of centrality within the uncertainties of the measurements. Unlike high- p_T charged hadrons measured by the ALICE Collaboration, W and Z

bosons show no indication of yield suppression in peripheral collisions.

Acknowledgements

We thank CERN for the very successful operation of the LHC, as well as the support staff from our institutions without whom ATLAS could not be operated efficiently.

We acknowledge the support of ANPCyT, Argentina; YerPhI, Armenia; ARC, Australia; BMWFW and FWF, Austria; ANAS, Azerbaijan; SSTC, Belarus; CNPq and FAPESP, Brazil; NSERC, NRC and CFI, Canada; CERN; CONICYT, Chile; CAS, MOST and NSFC, China; COLCIENCIAS, Colombia; MSMT CR, MPO CR and VSC CR, Czech Republic; DNRF and DNSRC, Denmark; IN2P3-CNRS, CEA-DRF/IRFU, France; SRNSFG, Georgia; BMBF, HGF, and MPG, Germany; GSRT, Greece; RGC, Hong Kong SAR, China; ISF and Benoziyo Center, Israel; INFN, Italy; MEXT and JSPS, Japan; CNRST, Morocco; NWO, Netherlands; RCN, Norway; MNiSW and NCN, Poland; FCT, Portugal; MNE/IFA, Romania; MES of Russia and NRC KI, Russian Federation; JINR; MESTD, Serbia; MSSR, Slovakia; ARRS and MIZŠ, Slovenia; DST/NRF, South Africa; MINECO, Spain; SRC and Wallenberg Foundation, Sweden; SERI, SNSF and Cantons of Bern and Geneva, Switzerland; MOST, Taiwan; TAEK, Turkey; STFC, United Kingdom; DOE and NSF, United States of America. In addition, individual groups and members have received support from BCKDF, CANARIE, CRC and Compute Canada, Canada; COST, ERC, ERDF, Horizon 2020, and Marie Skłodowska-Curie Actions, European Union; Investissements d'Avenir Labex and Idex, ANR, France; DFG and AvH Foundation, Germany; Herakleitos, Thales and Aristeia programmes cofinanced by EU-ESF and the Greek NSRF, Greece; BSF-NSF and GIF, Israel; CERCA Programme Generalitat de Catalunya, Spain; The Royal Society and Leverhulme Trust, United Kingdom.

The crucial computing support from all WLCG partners is acknowledged gratefully, in particular from CERN, the ATLAS Tier-1 facilities at TRIUMF (Canada), NDGF (Denmark, Norway, Sweden), CC-IN2P3 (France), KIT/GridKA (Germany), INFN-CNAF (Italy), NL-T1 (Netherlands), PIC (Spain), ASGC (Taiwan), RAL (UK) and BNL (USA), the Tier-2 facilities worldwide and large non-WLCG resource providers. Major contributors of computing resources are listed in Ref. [65].

References

- [1] ATLAS Collaboration, Measurement of Z boson production in Pb+Pb collisions at $\sqrt{s_{NN}} = 2.76$ TeV with the ATLAS detector, Phys. Rev. Lett. 110 (2013) 022301, arXiv:1210.6486 [hep-ex].
- [2] ATLAS Collaboration, Measurement of the production and lepton charge asymmetry of W bosons in Pb+Pb collisions at $\sqrt{s_{NN}} = 2.76$ TeV with the ATLAS detector, Eur. Phys. J. C 75 (2015) 23, arXiv:1408.4674 [hep-ex].
- [3] CMS Collaboration, Study of Z boson production in PbPb collisions at $\sqrt{s_{NN}} = 2.76$ TeV, Phys. Rev. Lett. 106 (2011) 212301, arXiv:1102.5435 [nucl-ex].
- [4] CMS Collaboration, Study of Z production in PbPb and pp collisions at $\sqrt{s_{NN}} = 2.76$ TeV in the dimuon and dielectron decay channels, J. High Energy Phys. 03 (2015) 022, arXiv:1410.4825 [nucl-ex].
- [5] CMS Collaboration, Study of W boson production in PbPb and pp collisions at $\sqrt{s_{NN}} = 2.76$ TeV, Phys. Lett. B 715 (2012) 66, arXiv:1205.6334 [nucl-ex].
- [6] ATLAS Collaboration, Measurement of W^\pm boson production in Pb+Pb collisions at $\sqrt{s_{NN}} = 5.02$ TeV with the ATLAS detector, Eur. Phys. J. C 79 (2019) 935, arXiv:1907.10414 [nucl-ex].
- [7] ATLAS Collaboration, Centrality, rapidity and transverse momentum dependence of isolated prompt photon production in lead-lead collisions at $\sqrt{s_{NN}} = 2.76$ TeV measured with the ATLAS detector, Phys. Rev. C 93 (2016) 034914, arXiv:1506.08552 [hep-ex].
- [8] CMS Collaboration, Measurement of isolated photon production in pp and PbPb collisions at $\sqrt{s_{NN}} = 2.76$ TeV, Phys. Lett. B 710 (2012) 256, arXiv:1201.3093 [nucl-ex].
- [9] ALICE Collaboration, Measurement of Z^0 -boson production at large rapidities in Pb-Pb collisions at $\sqrt{s_{NN}} = 5.02$ TeV, Phys. Lett. B 780 (2018) 372, arXiv:1711.10753 [nucl-ex].

- [10] LHCb Collaboration, Observation of Z production in proton-lead collisions at LHCb, *J. High Energy Phys.* 09 (2014) 030, arXiv:1406.2885 [hep-ex].
- [11] ATLAS Collaboration, Z boson production in p -Pb collisions at $\sqrt{s_{NN}} = 5.02$ TeV measured with the ATLAS detector, *Phys. Rev. C* 92 (2015) 044915, arXiv:1507.06232 [hep-ex].
- [12] CMS Collaboration, Study of Z boson production in pPb collisions at $\sqrt{s_{NN}} = 5.02$ TeV, *Phys. Lett. B* 759 (2016) 36, arXiv:1512.06461 [hep-ex].
- [13] ALICE Collaboration, W and Z boson production in p -Pb collisions at $\sqrt{s_{NN}} = 5.02$ TeV, *J. High Energy Phys.* 02 (2017) 077, arXiv:1611.03002 [nucl-ex].
- [14] CMS Collaboration, Observation of nuclear modifications in W^\pm boson production in pPb collisions at $\sqrt{s_{NN}} = 8.16$ TeV, arXiv:1905.01486 [hep-ex], 2019.
- [15] ATLAS Collaboration, Measurements of W and Z boson production in pp collisions at $\sqrt{s} = 5.02$ TeV with the ATLAS detector, *Eur. Phys. J. C* 79 (2019) 128, arXiv:1810.08424 [hep-ex], Erratum: *Eur. Phys. J. C* 79 (2019) 374.
- [16] ATLAS Collaboration, The ATLAS experiment at the CERN large hadron collider, *J. Instrum.* 3 (2008) S08003.
- [17] ATLAS Collaboration, ATLAS insertable B-layer technical design report, ATLAS-TDR-19, <https://cds.cern.ch/record/1291633>, 2010, Addendum: <https://cds.cern.ch/record/1451888>, 2012.
- [18] B. Abbott, et al., Production and integration of the ATLAS insertable B-layer, *J. Instrum.* 13 (2018) T05008, arXiv:1803.00844 [physics.ins-det].
- [19] ATLAS Collaboration, Performance of the ATLAS trigger system in 2015, *Eur. Phys. J. C* 77 (2017) 317, arXiv:1611.09661 [hep-ex].
- [20] ATLAS Collaboration, Performance of electron and photon triggers in ATLAS during LHC run 2, arXiv:1909.00761 [hep-ex], 2019.
- [21] ATLAS Collaboration, Measurement of the jet radius and transverse momentum dependence of inclusive jet suppression in lead-lead collisions at $\sqrt{s_{NN}} = 2.76$ TeV with the ATLAS detector, *Phys. Lett. B* 719 (2013) 220, arXiv:1208.1967 [hep-ex].
- [22] ATLAS Collaboration, Muon reconstruction performance of the ATLAS detector in proton-proton collision data at $\sqrt{s} = 13$ TeV, *Eur. Phys. J. C* 76 (2016) 292, arXiv:1603.05598 [hep-ex].
- [23] ATLAS Collaboration, Electron reconstruction and identification in the ATLAS experiment using the 2015 and 2016 LHC proton-proton collision data at $\sqrt{s} = 13$ TeV, *Eur. Phys. J. C* 79 (2019) 639, arXiv:1902.04655 [physics.ins-det].
- [24] M.L. Miller, K. Reygers, S.J. Sanders, P. Steinberg, Glauber modeling in high-energy nuclear collisions, *Annu. Rev. Nucl. Part. Sci.* 57 (2007) 205, arXiv:nucl-ex/0701025.
- [25] ATLAS Collaboration, Prompt and non-prompt J/ψ and $\psi(2S)$ suppression at high transverse momentum in 5.02 TeV Pb+Pb collisions with the ATLAS experiment, *Eur. Phys. J. C* 78 (2018) 762, arXiv:1805.04077 [nucl-ex].
- [26] ATLAS Collaboration, Measurement of photon-jet transverse momentum correlations in 5.02 TeV Pb+Pb and pp collisions with ATLAS, *Phys. Lett. B* 789 (2019) 167, arXiv:1809.07280 [nucl-ex].
- [27] S. Agostinelli, et al., GEANT4 - a simulation toolkit, *Nucl. Instrum. Methods A* 506 (2003) 250.
- [28] ATLAS Collaboration, The ATLAS simulation infrastructure, *Eur. Phys. J. C* 70 (2010) 823, arXiv:1005.4568 [physics.ins-det].
- [29] P. Nason, A new method for combining NLO QCD with shower Monte Carlo algorithms, *J. High Energy Phys.* 11 (2004) 040, arXiv:hep-ph/0409146 [hep-ph].
- [30] S. Frixione, P. Nason, C. Oleari, Matching NLO QCD computations with parton shower simulations: the POWHEG method, *J. High Energy Phys.* 11 (2007) 070, arXiv:0709.2092 [hep-ph].
- [31] S. Alioli, P. Nason, C. Oleari, E. Re, A general framework for implementing NLO calculations in shower Monte Carlo programs: the POWHEG BOX, *J. High Energy Phys.* 06 (2010) 043, arXiv:1002.2581 [hep-ph].
- [32] S. Alioli, P. Nason, C. Oleari, E. Re, NLO vector-boson production matched with shower in POWHEG, *J. High Energy Phys.* 07 (2008) 060, arXiv:0805.4802 [hep-ph].
- [33] T. Sjöstrand, S. Mrenna, P.Z. Skands, A brief introduction to PYTHIA 8.1, *Comput. Phys. Commun.* 178 (2008) 852, arXiv:0710.3820 [hep-ph].
- [34] J. Gao, et al., CT10 next-to-next-to-leading order global analysis of QCD, *Phys. Rev. D* 89 (2014) 033009, arXiv:1302.6246 [hep-ph].
- [35] J. Pumplin, et al., New generation of parton distributions with uncertainties from global QCD analysis, *J. High Energy Phys.* 07 (2002) 012, arXiv:hep-ph/0201195 [hep-ph].
- [36] ATLAS Collaboration, Measurement of the Z/γ^* boson transverse momentum distribution in pp collisions at $\sqrt{s} = 7$ TeV with the ATLAS detector, *J. High Energy Phys.* 09 (2014) 145, arXiv:1406.3660 [hep-ex].
- [37] N. Davidson, T. Przydzinski, Z. Was, PHOTOS interface in C++; technical and physics documentation, *Comput. Phys. Commun.* 199 (2016) 86, arXiv:1011.0937 [hep-ph].
- [38] S. Frixione, P. Nason, G. Ridolfi, A positive-weight next-to-leading-order Monte Carlo for heavy flavour hadroproduction, *J. High Energy Phys.* 09 (2007) 126, arXiv:0707.3088 [hep-ph].
- [39] H.-L. Lai, et al., New parton distributions for collider physics, *Phys. Rev. D* 82 (2010) 074024, arXiv:1007.2241 [hep-ph].
- [40] T. Sjöstrand, S. Mrenna, P.Z. Skands, PYTHIA 6.4 physics and manual, *J. High Energy Phys.* 05 (2006) 026, arXiv:hep-ph/0603175 [hep-ph].
- [41] P.Z. Skands, Tuning Monte Carlo generators: the Perugia tunes, *Phys. Rev. D* 82 (2010) 074018, arXiv:1005.3457 [hep-ph].
- [42] D.J. Lange, The EvtGen particle decay simulation package, *Nucl. Instrum. Methods A* 462 (2001) 152.
- [43] ATLAS Collaboration, Electron and photon energy calibration with the ATLAS detector using 2015-2016 LHC proton-proton collision data, *J. Instrum.* 14 (2019) P03017, arXiv:1812.03848 [hep-ex].
- [44] C.A. Bertulani, G. Baur, Electromagnetic processes in relativistic heavy ion collisions, *Phys. Rep.* 163 (1988) 299.
- [45] F. Krauss, M. Greiner, G. Soff, Photon and gluon induced processes in relativistic heavy ion collisions, *Prog. Part. Nucl. Phys.* 39 (1997) 503.
- [46] G. Baur, Coherent photon-photon interactions in very peripheral relativistic heavy ion collisions, *Eur. Phys. J. D* 55 (2009) 265, arXiv:0810.1400 [nucl-th].
- [47] V.P. Gonçalves, M.V.T. Machado, Diffractive photoproduction of Z^0 bosons in coherent interactions at CERN-LHC, *Eur. Phys. J. C* 56 (2008) 33, arXiv:0710.4287 [hep-ph], Erratum: *Eur. Phys. J. C* 61 (2009) 351.
- [48] ATLAS Collaboration, Measurement of exclusive $\gamma\gamma \rightarrow \ell^+\ell^-$ production in proton-proton collisions at $\sqrt{s} = 7$ TeV with the ATLAS detector, *Phys. Lett. B* 749 (2015) 242, arXiv:1506.07098 [hep-ex].
- [49] CMS Collaboration, Exclusive photon-photon production of muon pairs in proton-proton collisions at $\sqrt{s} = 7$ TeV, *J. High Energy Phys.* 01 (2012) 052, arXiv:1111.5536 [hep-ex].
- [50] ATLAS Collaboration, Rapidity gap cross sections measured with the ATLAS detector in pp collisions at $\sqrt{s} = 7$ TeV, *Eur. Phys. J. C* 72 (2012) 1926, arXiv:1201.2808 [hep-ex].
- [51] ATLAS Collaboration, Observation of centrality-dependent acoplanarity for muon pairs produced via two-photon scattering in Pb+Pb collisions at $\sqrt{s_{NN}} = 5.02$ TeV with the ATLAS detector, *Phys. Rev. Lett.* 121 (2018) 212301, arXiv:1806.08708 [nucl-ex].
- [52] A. Valassi, Combining correlated measurements of several different physical quantities, *Nucl. Instrum. Methods A* 500 (2003) 391.
- [53] S. Catani, M. Grazzini, Next-to-next-to-leading order subtraction formalism in hadron collisions and its application to Higgs boson production at the Large Hadron Collider, *Phys. Rev. Lett.* 98 (2007) 222002, arXiv:hep-ph/0703012 [hep-ph].
- [54] S. Catani, L. Cieri, G. Ferrera, D. de Florian, M. Grazzini, Vector boson production at hadron colliders: a fully exclusive QCD calculation at next-to-next-to-leading order, *Phys. Rev. Lett.* 103 (2009) 082001, arXiv:0903.2120 [hep-ph].
- [55] W.F.L. Hollik, Radiative corrections in the standard model and their rôle for precision tests of the electroweak theory, *Fortschr. Phys.* 38 (1990) 165.
- [56] Particle Data Group, K.A. Olive, et al., Review of particle physics, *Chin. Phys. C* 38 (2014) 090001.
- [57] S. Dulat, et al., New parton distribution functions from a global analysis of quantum chromodynamics, *Phys. Rev. D* 93 (2016) 033006, arXiv:1506.07443 [hep-ph].
- [58] K. Kovarik, et al., nCTEQ15 - global analysis of nuclear parton distributions with uncertainties in the CTEQ framework, *Phys. Rev. D* 93 (2016) 085037, arXiv:1509.00792 [hep-ph].
- [59] K.J. Eskola, P. Paakkinen, H. Paukkunen, C.A. Salgado, EPPS16: nuclear parton distributions with LHC data, *Eur. Phys. J. C* 77 (2017) 163, arXiv:1612.05741 [hep-ph].
- [60] J.M. Campbell, R.K. Ellis, W.T. Giele, A multi-threaded version of MCFM, *Eur. Phys. J. C* 75 (2015) 246, arXiv:1503.06182 [physics.comp-ph].
- [61] C. Loizides, J. Kamin, D. d'Enterria, Improved Monte Carlo Glauber predictions at present and future nuclear colliders, *Phys. Rev. C* 97 (2018) 054910, arXiv:1710.07098 [nucl-ex], Erratum: *Phys. Rev. C* 99 (2019) 019901.
- [62] ALICE Collaboration, Analysis of the apparent nuclear modification in peripheral Pb-Pb collisions at 5.02 TeV, *Phys. Lett. B* 793 (2019) 420, arXiv:1805.05212 [nucl-ex].
- [63] C. Loizides, A. Morsch, Absence of jet quenching in peripheral nucleus-nucleus collisions, *Phys. Lett. B* 773 (2017) 408, arXiv:1705.08856 [nucl-ex].
- [64] X.-N. Wang, M. Gyulassy, HIJING: a Monte Carlo model for multiple jet production in pp , pA and AA collisions, *Phys. Rev. D* 44 (1991) 3501.
- [65] ATLAS Collaboration, ATLAS computing acknowledgements, ATL-GEN-PUB-2016-002, <https://cds.cern.ch/record/2202407>.

The ATLAS Collaboration

G. Aad ¹⁰¹, B. Abbott ¹²⁸, D.C. Abbott ¹⁰², A. Abed Abud ^{70a,70b}, K. Abeling ⁵³, D.K. Abhayasinghe ⁹³, S.H. Abidi ¹⁶⁷, O.S. AbouZeid ⁴⁰, N.L. Abraham ¹⁵⁶, H. Abramowicz ¹⁶¹, H. Abreu ¹⁶⁰, Y. Abulaiti ⁶, B.S. Acharya ^{66a,66b,o}, B. Achkar ⁵³, S. Adachi ¹⁶³, L. Adam ⁹⁹, C. Adam Bourdarios ⁵, L. Adamczyk ^{83a}, L. Adamek ¹⁶⁷, J. Adelman ¹²⁰, M. Adersberger ¹¹³, A. Adiguzel ^{12c}, S. Adorni ⁵⁴, T. Adye ¹⁴⁴, A.A. Affolder ¹⁴⁶, Y. Afik ¹⁶⁰, C. Agapopoulou ¹³², M.N. Agaras ³⁸, A. Aggarwal ¹¹⁸, C. Agheorghiesei ^{27c}, J.A. Aguilar-Saavedra ^{140f,140a,ai}, F. Ahmadov ⁷⁹, W.S. Ahmed ¹⁰³, X. Ai ¹⁸, G. Aielli ^{73a,73b}, S. Akatsuka ⁸⁵, T.P.A. Åkesson ⁹⁶, E. Akilli ⁵⁴, A.V. Akimov ¹¹⁰, K. Al Khoury ¹³², G.L. Alberghi ^{23b,23a}, J. Albert ¹⁷⁶, M.J. Alconada Verzini ¹⁶¹, S. Alderweireldt ³⁶, M. Aleksa ³⁶, I.N. Aleksandrov ⁷⁹, C. Alexa ^{27b}, D. Alexandre ¹⁹, T. Alexopoulos ¹⁰, A. Alfonsi ¹¹⁹, F. Alfonsi ^{23b,23a}, M. Alhroob ¹²⁸, B. Ali ¹⁴², G. Alimonti ^{68a}, J. Alison ³⁷, S.P. Alkire ¹⁴⁸, C. Allaire ¹³², B.M.M. Allbrooke ¹⁵⁶, B.W. Allen ¹³¹, P.P. Allport ²¹, A. Aloisio ^{69a,69b}, A. Alonso ⁴⁰, F. Alonso ⁸⁸, C. Alpigiani ¹⁴⁸, A.A. Alshehri ⁵⁷, M. Alvarez Estevez ⁹⁸, D. Álvarez Piqueras ¹⁷⁴, M.G. Alviggi ^{69a,69b}, Y. Amaral Coutinho ^{80b}, A. Ambler ¹⁰³, L. Ambroz ¹³⁵, C. Amelung ²⁶, D. Amidei ¹⁰⁵, S.P. Amor Dos Santos ^{140a}, S. Amoroso ⁴⁶, C.S. Amrouche ⁵⁴, F. An ⁷⁸, C. Anastopoulos ¹⁴⁹, N. Andari ¹⁴⁵, T. Andeen ¹¹, C.F. Anders ^{61b}, J.K. Anders ²⁰, A. Andreazza ^{68a,68b}, V. Andrei ^{61a}, C.R. Anelli ¹⁷⁶, S. Angelidakis ³⁸, A. Angerami ³⁹, A.V. Anisenkov ^{121b,121a}, A. Annovi ^{71a}, C. Antel ^{61a}, M.T. Anthony ¹⁴⁹, E. Antipov ¹²⁹, M. Antonelli ⁵¹, D.J.A. Antrim ¹⁷¹, F. Anulli ^{72a}, M. Aoki ⁸¹, J.A. Aparisi Pozo ¹⁷⁴, L. Aperio Bella ^{15a}, G. Arabidze ¹⁰⁶, J.P. Araque ^{140a}, V. Araujo Ferraz ^{80b}, R. Araujo Pereira ^{80b}, C. Arcangeletti ⁵¹, A.T.H. Arce ⁴⁹, F.A. Arduh ⁸⁸, J.-F. Arguin ¹⁰⁹, S. Argyropoulos ⁷⁷, J.-H. Arling ⁴⁶, A.J. Armbruster ³⁶, A. Armstrong ¹⁷¹, O. Arnaez ¹⁶⁷, H. Arnold ¹¹⁹, Z.P. Arrubarrena Tame ¹¹³, A. Artamonov ^{123,*}, G. Artoni ¹³⁵, S. Artz ⁹⁹, S. Asai ¹⁶³, N. Asbah ⁵⁹, E.M. Asimakopoulou ¹⁷², L. Asquith ¹⁵⁶, J. Assahsah ^{35d}, K. Assamagan ²⁹, R. Astalos ^{28a}, R.J. Atkin ^{33a}, M. Atkinson ¹⁷³, N.B. Atlay ¹⁹, H. Atmani ¹³², K. Augsten ¹⁴², G. Avolio ³⁶, R. Avramidou ^{60a}, M.K. Ayoub ^{15a}, A.M. Azoulay ^{168b}, G. Azuelos ^{109,ax}, H. Bachacou ¹⁴⁵, K. Bachas ^{67a,67b}, M. Backes ¹³⁵, F. Backman ^{45a,45b}, P. Bagnaia ^{72a,72b}, M. Bahmani ⁸⁴, H. Bahrsemani ¹⁵², A.J. Bailey ¹⁷⁴, V.R. Bailey ¹⁷³, J.T. Baines ¹⁴⁴, M. Bajic ⁴⁰, C. Bakalis ¹⁰, O.K. Baker ¹⁸³, P.J. Bakker ¹¹⁹, D. Bakshi Gupta ⁸, S. Balaji ¹⁵⁷, E.M. Baldin ^{121b,121a}, P. Balek ¹⁸⁰, F. Balli ¹⁴⁵, W.K. Balunas ¹³⁵, J. Balz ⁹⁹, E. Banas ⁸⁴, A. Bandyopadhyay ²⁴, Sw. Banerjee ^{181,j}, A.A.E. Bannoura ¹⁸², L. Barak ¹⁶¹, W.M. Barbe ³⁸, E.L. Barberio ¹⁰⁴, D. Barberis ^{55b,55a}, M. Barbero ¹⁰¹, G. Barbour ⁹⁴, T. Barillari ¹¹⁴, M.-S. Barisits ³⁶, J. Barkeloo ¹³¹, T. Barklow ¹⁵³, R. Barnea ¹⁶⁰, S.L. Barnes ^{60c}, B.M. Barnett ¹⁴⁴, R.M. Barnett ¹⁸, Z. Barnovska-Blenessy ^{60a}, A. Baroncelli ^{60a}, G. Barone ²⁹, A.J. Barr ¹³⁵, L. Barranco Navarro ^{45a,45b}, F. Barreiro ⁹⁸, J. Barreiro Guimarães da Costa ^{15a}, S. Barsov ¹³⁸, R. Bartoldus ¹⁵³, G. Bartolini ¹⁰¹, A.E. Barton ⁸⁹, P. Bartos ^{28a}, A. Basalaev ⁴⁶, A. Bassalat ^{132,aq}, M.J. Basso ¹⁶⁷, R.L. Bates ⁵⁷, S. Batlamous ^{35e}, J.R. Batley ³², B. Batool ¹⁵¹, M. Battaglia ¹⁴⁶, M. Baue ^{72a,72b}, F. Bauer ¹⁴⁵, K.T. Bauer ¹⁷¹, H.S. Bawa ^{31,m}, J.B. Beacham ⁴⁹, T. Beau ¹³⁶, P.H. Beauchemin ¹⁷⁰, F. Becherer ⁵², P. Bechtel ²⁴, H.C. Beck ⁵³, H.P. Beck ^{20,s}, K. Becker ⁵², M. Becker ⁹⁹, C. Becot ⁴⁶, A. Beddall ^{12d}, A.J. Beddall ^{12a}, V.A. Bednyakov ⁷⁹, M. Bedognetti ¹¹⁹, C.P. Bee ¹⁵⁵, T.A. Beermann ¹⁸², M. Begalli ^{80b}, M. Begel ²⁹, A. Behera ¹⁵⁵, J.K. Behr ⁴⁶, F. Beisiegel ²⁴, A.S. Bell ⁹⁴, G. Bella ¹⁶¹, L. Bellagamba ^{23b}, A. Bellerive ³⁴, P. Bellos ⁹, K. Beloborodov ^{121b,121a}, K. Belotskiy ¹¹¹, N.L. Belyaev ¹¹¹, D. Benckekroun ^{35a}, N. Benekos ¹⁰, Y. Benhammou ¹⁶¹, D.P. Benjamin ⁶, M. Benoit ⁵⁴, J.R. Bensinger ²⁶, S. Bentvelsen ¹¹⁹, L. Beresford ¹³⁵, M. Beretta ⁵¹, D. Berge ⁴⁶, E. Bergeas Kuutmann ¹⁷², N. Berger ⁵, B. Bergmann ¹⁴², L.J. Bergsten ²⁶, J. Beringer ¹⁸, S. Berlendis ⁷, G. Bernardi ¹³⁶, C. Bernius ¹⁵³, F.U. Bernlochner ²⁴, T. Berry ⁹³, P. Berta ⁹⁹, C. Bertella ^{15a}, I.A. Bertram ⁸⁹, O. Bessidskaia Bylund ¹⁸², N. Besson ¹⁴⁵, A. Bethani ¹⁰⁰, S. Bethke ¹¹⁴, A. Betti ⁴², A.J. Bevan ⁹², J. Beyer ¹¹⁴, D.S. Bhattacharya ¹⁷⁷, P. Bhattarai ²⁶, R. Bi ¹³⁹, R.M. Bianchi ¹³⁹, O. Biebel ¹¹³, D. Biedermann ¹⁹, R. Bielski ³⁶, K. Bierwagen ⁹⁹, N.V. Biesuz ^{71a,71b}, M. Biglietti ^{74a}, T.R.V. Billoud ¹⁰⁹, M. Bindi ⁵³, A. Bingul ^{12d}, C. Bini ^{72a,72b}, S. Biondi ^{23b,23a}, M. Birman ¹⁸⁰, T. Bisanz ⁵³, J.P. Biswal ¹⁶¹, D. Biswas ^{181,j}, A. Bitadze ¹⁰⁰, C. Bittrich ⁴⁸, K. Björke ¹³⁴, K.M. Black ²⁵, T. Blazek ^{28a}, I. Bloch ⁴⁶, C. Blocker ²⁶, A. Blue ⁵⁷, U. Blumenschein ⁹², G.J. Bobbink ¹¹⁹, V.S. Bobrovnikov ^{121b,121a}, S.S. Bocchetta ⁹⁶, A. Bocci ⁴⁹, D. Boerner ⁴⁶, D. Bogavac ¹⁴, A.G. Bogdanchikov ^{121b,121a}, C. Boehm ^{45a}, V. Boisvert ⁹³, P. Bokan ^{53,172}, T. Bold ^{83a}, A.S. Boldyrev ¹¹², A.E. Bolz ^{61b}, M. Bomben ¹³⁶, M. Bona ⁹², J.S. Bonilla ¹³¹, M. Boonekamp ¹⁴⁵, C.D. Booth ⁹³, H.M. Borecka-Bielska ⁹⁰, A. Borisov ¹²², G. Borissov ⁸⁹, J. Bortfeldt ³⁶, D. Bortoletto ¹³⁵, D. Boscherini ^{23b},

M. Bosman¹⁴, J.D. Bossio Sola¹⁰³, K. Bouaouda^{35a}, J. Boudreau¹³⁹, E.V. Bouhova-Thacker⁸⁹, D. Boumediene³⁸, S.K. Boutle⁵⁷, A. Boveia¹²⁶, J. Boyd³⁶, D. Boye^{33b,ar}, I.R. Boyko⁷⁹, A.J. Bozson⁹³, J. Bracinik²¹, N. Brahimi¹⁰¹, G. Brandt¹⁸², O. Brandt³², F. Braren⁴⁶, B. Brau¹⁰², J.E. Brau¹³¹, W.D. Breaden Madden⁵⁷, K. Brendlinger⁴⁶, L. Brenner⁴⁶, R. Brenner¹⁷², S. Bressler¹⁸⁰, B. Brickwedde⁹⁹, D.L. Briglin²¹, D. Britton⁵⁷, D. Britzger¹¹⁴, I. Brock²⁴, R. Brock¹⁰⁶, G. Brooijmans³⁹, W.K. Brooks^{147c}, E. Brost¹²⁰, J.H. Broughton²¹, P.A. Bruckman de Renstrom⁸⁴, D. Bruncko^{28b}, A. Bruni^{23b}, G. Bruni^{23b}, L.S. Bruni¹¹⁹, S. Bruno^{73a,73b}, M. Bruschi^{23b}, N. Bruscino¹³⁹, P. Bryant³⁷, L. Bryngemark⁹⁶, T. Buanes¹⁷, Q. Buat³⁶, P. Buchholz¹⁵¹, A.G. Buckley⁵⁷, I.A. Budagov⁷⁹, M.K. Bugge¹³⁴, F. Bühner⁵², O. Bulekov¹¹¹, T.J. Burch¹²⁰, S. Burdin⁹⁰, C.D. Burgard¹¹⁹, A.M. Burger¹²⁹, B. Burghgrave⁸, J.T.P. Burr⁴⁶, C.D. Burton¹¹, J.C. Burzynski¹⁰², V. Büscher⁹⁹, E. Buschmann⁵³, P.J. Bussey⁵⁷, J.M. Butler²⁵, C.M. Buttar⁵⁷, J.M. Butterworth⁹⁴, P. Butti³⁶, W. Buttinger³⁶, C.J. Buxo Vazquez¹⁰⁶, A. Buzatu¹⁵⁸, A.R. Buzykaev^{121b,121a}, G. Cabras^{23b,23a}, S. Cabrera Urbán¹⁷⁴, D. Caforio⁵⁶, H. Cai¹⁷³, V.M.M. Cairo¹⁵³, O. Cakir^{4a}, N. Calace³⁶, P. Calafiura¹⁸, A. Calandri¹⁰¹, G. Calderini¹³⁶, P. Calfayan⁶⁵, G. Callea⁵⁷, L.P. Caloba^{80b}, S. Calvente Lopez⁹⁸, D. Calvet³⁸, S. Calvet³⁸, T.P. Calvet¹⁵⁵, M. Calvetti^{71a,71b}, R. Camacho Toro¹³⁶, S. Camarda³⁶, D. Camarero Munoz⁹⁸, P. Camarri^{73a,73b}, D. Cameron¹³⁴, R. Caminal Armadans¹⁰², C. Camincher³⁶, S. Campana³⁶, M. Campanelli⁹⁴, A. Camplani⁴⁰, A. Campoverde¹⁵¹, V. Canale^{69a,69b}, A. Canesse¹⁰³, M. Cano Bret^{60c}, J. Cantero¹²⁹, T. Cao¹⁶¹, Y. Cao¹⁷³, M.D.M. Capeans Garrido³⁶, M. Capua^{41b,41a}, R. Cardarelli^{73a}, F. Cardillo¹⁴⁹, G. Carducci^{41b,41a}, I. Carli¹⁴³, T. Carli³⁶, G. Carlino^{69a}, B.T. Carlson¹³⁹, L. Carminati^{68a,68b}, R.M.D. Carney^{45a,45b}, S. Caron¹¹⁸, E. Carquin^{147c}, S. Carrá⁴⁶, J.W.S. Carter¹⁶⁷, M.P. Casado^{14,e}, A.F. Casha¹⁶⁷, D.W. Casper¹⁷¹, R. Castelijns¹¹⁹, F.L. Castillo¹⁷⁴, V. Castillo Gimenez¹⁷⁴, N.F. Castro^{140a,140e}, A. Catinaccio³⁶, J.R. Catmore¹³⁴, A. Cattai³⁶, J. Caudron²⁴, V. Cavaliere²⁹, E. Cavallaro¹⁴, M. Cavalli-Sforza¹⁴, V. Cavasinni^{71a,71b}, E. Celebi^{12b}, F. Ceradini^{74a,74b}, L. Cerda Alberich¹⁷⁴, K. Cerny¹³⁰, A.S. Cerqueira^{80a}, A. Cerri¹⁵⁶, L. Cerrito^{73a,73b}, F. Cerutti¹⁸, A. Cervelli^{23b,23a}, S.A. Cetin^{12b}, Z. Chadi^{35a}, D. Chakraborty¹²⁰, S.K. Chan⁵⁹, W.S. Chan¹¹⁹, W.Y. Chan⁹⁰, J.D. Chapman³², B. Chargeishvili^{159b}, D.G. Charlton²¹, T.P. Charman⁹², C.C. Chau³⁴, S. Che¹²⁶, S. Chekanov⁶, S.V. Chekulaev^{168a}, G.A. Chelkov^{79,aw}, M.A. Chelstowska³⁶, B. Chen⁷⁸, C. Chen^{60a}, C.H. Chen⁷⁸, H. Chen²⁹, J. Chen^{60a}, J. Chen³⁹, S. Chen¹³⁷, S.J. Chen^{15c}, X. Chen^{15b,av}, Y. Chen⁸², Y.-H. Chen⁴⁶, H.C. Cheng^{63a}, H.J. Cheng^{15a}, A. Cheplakov⁷⁹, E. Cheremushkina¹²², R. Cherkaoui El Moursli^{35e}, E. Cheu⁷, K. Cheung⁶⁴, T.J.A. Chevaléras¹⁴⁵, L. Chevalier¹⁴⁵, V. Chiarella⁵¹, G. Chiarelli^{71a}, G. Chiodini^{67a}, A.S. Chisholm²¹, A. Chitan^{27b}, I. Chiu¹⁶³, Y.H. Chiu¹⁷⁶, M.V. Chizhov⁷⁹, K. Choi⁶⁵, A.R. Chomont^{72a,72b}, S. Chouridou¹⁶², Y.S. Chow¹¹⁹, M.C. Chu^{63a}, X. Chu^{15a,15d}, J. Chudoba¹⁴¹, A.J. Chuinard¹⁰³, J.J. Chwastowski⁸⁴, L. Chytka¹³⁰, D. Cieri¹¹⁴, K.M. Ciesla⁸⁴, D. Cinca⁴⁷, V. Cindro⁹¹, I.A. Cioară^{27b}, A. Ciochio¹⁸, F. Ciotto^{69a,69b}, Z.H. Citron^{180,k}, M. Citterio^{68a}, D.A. Ciubotaru^{27b}, B.M. Ciungu¹⁶⁷, A. Clark⁵⁴, M.R. Clark³⁹, P.J. Clark⁵⁰, C. Clement^{45a,45b}, Y. Coadou¹⁰¹, M. Cobal^{66a,66c}, A. Coccaro^{55b}, J. Cochran⁷⁸, H. Cohen¹⁶¹, A.E.C. Coimbra³⁶, L. Colasurdo¹¹⁸, B. Cole³⁹, A.P. Colijn¹¹⁹, J. Collot⁵⁸, P. Conde Muñio^{140a,f}, E. Coniavitis⁵², S.H. Connell^{33b}, I.A. Connolly⁵⁷, S. Constantinescu^{27b}, F. Conventi^{69a,ay}, A.M. Cooper-Sarkar¹³⁵, F. Cormier¹⁷⁵, K.J.R. Cormier¹⁶⁷, L.D. Corpe⁹⁴, M. Corradi^{72a,72b}, E.E. Corrigan⁹⁶, F. Corriveau^{103,ae}, A. Cortes-Gonzalez³⁶, M.J. Costa¹⁷⁴, F. Costanza⁵, D. Costanzo¹⁴⁹, G. Cowan⁹³, J.W. Cowley³², J. Crane¹⁰⁰, K. Cranmer¹²⁴, S.J. Crawley⁵⁷, R.A. Creager¹³⁷, S. Crépé-Renaudin⁵⁸, F. Crescioli¹³⁶, M. Cristinziani²⁴, V. Croft¹¹⁹, G. Crosetti^{41b,41a}, A. Cueto⁵, T. Cuhadar Donszelmann¹⁴⁹, A.R. Cukierman¹⁵³, W.R. Cunningham⁵⁷, S. Czekierda⁸⁴, P. Czodrowski³⁶, M.J. Da Cunha Sargedas De Sousa^{60b}, J.V. Da Fonseca Pinto^{80b}, C. Da Via¹⁰⁰, W. Dabrowski^{83a}, T. Dado^{28a}, S. Dahbi^{35e}, T. Dai¹⁰⁵, C. Dallapiccola¹⁰², M. Dam⁴⁰, G. D'amen²⁹, V. D'Amico^{74a,74b}, J. Damp⁹⁹, J.R. Dandoy¹³⁷, M.F. Daneri³⁰, N.P. Dang^{181,j}, N.S. Dann¹⁰⁰, M. Danninger¹⁷⁵, V. Dao³⁶, G. Darbo^{55b}, O. Dartsis⁵, A. Dattagupta¹³¹, T. Daubney⁴⁶, S. D'Auria^{68a,68b}, W. Davey²⁴, C. David⁴⁶, T. Davidek¹⁴³, D.R. Davis⁴⁹, I. Dawson¹⁴⁹, K. De⁸, R. De Asmundis^{69a}, M. De Beurs¹¹⁹, S. De Castro^{23b,23a}, S. De Cecco^{72a,72b}, N. De Groot¹¹⁸, P. de Jong¹¹⁹, H. De la Torre¹⁰⁶, A. De Maria^{15c}, D. De Pedis^{72a}, A. De Salvo^{72a}, U. De Sanctis^{73a,73b}, M. De Santis^{73a,73b}, A. De Santo¹⁵⁶, K. De Vasconcelos Corga¹⁰¹, J.B. De Vivie De Regie¹³², C. Debenedetti¹⁴⁶, D.V. Dedovich⁷⁹, A.M. Deiana⁴², M. Del Gaudio^{41b,41a}, J. Del Peso⁹⁸, Y. Delabat Diaz⁴⁶, D. Delgove¹³², F. Deliot^{145,r}, C.M. Delitzsch⁷, M. Della Pietra^{69a,69b}, D. Della Volpe⁵⁴, A. Dell'Acqua³⁶, L. Dell'Asta^{73a,73b},

M. Delmastro⁵, C. Delporte¹³², P.A. Delsart⁵⁸, D.A. DeMarco¹⁶⁷, S. Demers¹⁸³, M. Demichev⁷⁹, G. Demontigny¹⁰⁹, S.P. Denisov¹²², D. Denysiuk¹¹⁹, L. D'Eramo¹³⁶, D. Derendarz⁸⁴, J.E. Derkaoui^{35d}, F. Derue¹³⁶, P. Dervan⁹⁰, K. Desch²⁴, C. Deterre⁴⁶, K. Dette¹⁶⁷, C. Deutsch²⁴, M.R. Devesa³⁰, P.O. Deviveiros³⁶, A. Dewhurst¹⁴⁴, F.A. Di Bello⁵⁴, A. Di Ciaccio^{73a,73b}, L. Di Ciaccio⁵, W.K. Di Clemente¹³⁷, C. Di Donato^{69a,69b}, A. Di Girolamo³⁶, G. Di Gregorio^{71a,71b}, B. Di Micco^{74a,74b}, R. Di Nardo¹⁰², K.F. Di Petrillo⁵⁹, R. Di Sipio¹⁶⁷, D. Di Valentino³⁴, C. Diaconu¹⁰¹, F.A. Dias⁴⁰, T. Dias Do Vale^{140a}, M.A. Diaz^{147a}, J. Dickinson¹⁸, E.B. Diehl¹⁰⁵, J. Dietrich¹⁹, S. Díez Cornell⁴⁶, A. Dimitrievska¹⁸, W. Ding^{15b}, J. Dingfelder²⁴, F. Dittus³⁶, F. Djama¹⁰¹, T. Djobava^{159b}, J.I. Djuvsland¹⁷, M.A.B. Do Vale^{80c}, M. Dobre^{27b}, D. Dodsworth²⁶, C. Doglioni⁹⁶, J. Dolejsi¹⁴³, Z. Dolezal¹⁴³, M. Donadelli^{80d}, B. Dong^{60c}, J. Donini³⁸, A. D'Onofrio⁹², M. D'Onofrio⁹⁰, J. Dopke¹⁴⁴, A. Doria^{69a}, M.T. Dova⁸⁸, A.T. Doyle⁵⁷, E. Drechsler¹⁵², E. Dreyer¹⁵², T. Dreyer⁵³, A.S. Drobac¹⁷⁰, D. Du^{60b}, Y. Duan^{60b}, F. Dubinin¹¹⁰, M. Dubovsky^{28a}, A. Dubreuil⁵⁴, E. Duchovni¹⁸⁰, G. Duckeck¹¹³, A. Ducourthial¹³⁶, O.A. Ducu¹⁰⁹, D. Duda¹¹⁴, A. Dudarev³⁶, A.C. Dudder⁹⁹, E.M. Duffield¹⁸, L. Duflot¹³², M. Dührssen³⁶, C. Dülken¹⁸², M. Dumancic¹⁸⁰, A.E. Dumitriu^{27b}, A.K. Duncan⁵⁷, M. Dunford^{61a}, A. Duperrin¹⁰¹, H. Duran Yildiz^{4a}, M. Düren⁵⁶, A. Durglishvili^{159b}, D. Duschinger⁴⁸, B. Dutta⁴⁶, D. Duvnjak¹, G.I. Dyckes¹³⁷, M. Dyndal³⁶, S. Dysch¹⁰⁰, B.S. Dziedzic⁸⁴, K.M. Ecker¹¹⁴, R.C. Edgar¹⁰⁵, M.G. Eggleston⁴⁹, T. Eifert³⁶, G. Eigen¹⁷, K. Einsweiler¹⁸, T. Ekelof¹⁷², H. El Jarrari^{35e}, M. El Kacimi^{35c}, R. El Kosseifi¹⁰¹, V. Ellajosyula¹⁷², M. Ellert¹⁷², F. Ellinghaus¹⁸², A.A. Elliot⁹², N. Ellis³⁶, J. Elmsheuser²⁹, M. Elsing³⁶, D. Emelianov¹⁴⁴, A. Emerman³⁹, Y. Enari¹⁶³, M.B. Epland⁴⁹, J. Erdmann⁴⁷, A. Ereditato²⁰, M. Errenst³⁶, M. Escalier¹³², C. Escobar¹⁷⁴, O. Estrada Pastor¹⁷⁴, E. Etzion¹⁶¹, H. Evans⁶⁵, A. Ezhilov¹³⁸, F. Fabbri⁵⁷, L. Fabbri^{23b,23a}, V. Fabiani¹¹⁸, G. Facini⁹⁴, R.M. Faisca Rodrigues Pereira^{140a}, R.M. Fakhruddinov¹²², S. Falciano^{72a}, P.J. Falke⁵, S. Falke⁵, J. Faltova¹⁴³, Y. Fang^{15a}, Y. Fang^{15a}, G. Fanourakis⁴⁴, M. Fanti^{68a,68b}, M. Faraj^{66a,66c,u}, A. Farbin⁸, A. Farilla^{74a}, E.M. Farina^{70a,70b}, T. Farooque¹⁰⁶, S. Farrell¹⁸, S.M. Farrington⁵⁰, P. Farthouat³⁶, F. Fassi^{35e}, P. Fassnacht³⁶, D. Fassouliotis⁹, M. Fauci Giannelli⁵⁰, W.J. Fawcett³², L. Fayard¹³², O.L. Fedin^{138,p}, W. Fedorko¹⁷⁵, M. Feickert⁴², L. Feligioni¹⁰¹, A. Fell¹⁴⁹, C. Feng^{60b}, E.J. Feng³⁶, M. Feng⁴⁹, M.J. Fenton⁵⁷, A.B. Fenyuk¹²², J. Ferrando⁴⁶, A. Ferrante¹⁷³, A. Ferrari¹⁷², P. Ferrari¹¹⁹, R. Ferrari^{70a}, D.E. Ferreira de Lima^{61b}, A. Ferrer¹⁷⁴, D. Ferrere⁵⁴, C. Ferretti¹⁰⁵, F. Fiedler⁹⁹, A. Filipčič⁹¹, F. Filthaut¹¹⁸, K.D. Finelli²⁵, M.C.N. Fiolhais^{140a,140c,a}, L. Fiorini¹⁷⁴, F. Fischer¹¹³, W.C. Fisher¹⁰⁶, I. Fleck¹⁵¹, P. Fleischmann¹⁰⁵, R.R.M. Fletcher¹³⁷, T. Flick¹⁸², B.M. Flierl¹¹³, L. Flores¹³⁷, L.R. Flores Castillo^{63a}, F.M. Follega^{75a,75b}, N. Fomin¹⁷, J.H. Foo¹⁶⁷, G.T. Forcolin^{75a,75b}, A. Formica¹⁴⁵, F.A. Förster¹⁴, A.C. Forti¹⁰⁰, A.G. Foster²¹, M.G. Foti¹³⁵, D. Fournier¹³², H. Fox⁸⁹, P. Francavilla^{71a,71b}, S. Francescato^{72a,72b}, M. Franchini^{23b,23a}, S. Franchino^{61a}, D. Francis³⁶, L. Franconi²⁰, M. Franklin⁵⁹, A.N. Fray⁹², P.M. Freeman²¹, B. Freund¹⁰⁹, W.S. Freund^{80b}, E.M. Freundlich⁴⁷, D.C. Frizzell¹²⁸, D. Froidevaux³⁶, J.A. Frost¹³⁵, C. Fukunaga¹⁶⁴, E. Fullana Torregrosa¹⁷⁴, E. Fumagalli^{55b,55a}, T. Fusayasu¹¹⁵, J. Fuster¹⁷⁴, A. Gabrielli^{23b,23a}, A. Gabrielli¹⁸, G.P. Gach^{83a}, S. Gadatsch⁵⁴, P. Gadow¹¹⁴, G. Gagliardi^{55b,55a}, L.G. Gagnon¹⁰⁹, C. Galea^{27b}, B. Galhardo^{140a}, G.E. Gallardo¹³⁵, E.J. Gallas¹³⁵, B.J. Gallop¹⁴⁴, G. Galster⁴⁰, R. Gamboa Goni⁹², K.K. Gan¹²⁶, S. Ganguly¹⁸⁰, J. Gao^{60a}, Y. Gao⁵⁰, Y.S. Gao^{31,m}, C. García¹⁷⁴, J.E. García Navarro¹⁷⁴, J.A. García Pascual^{15a}, C. Garcia-Argos⁵², M. Garcia-Sciveres¹⁸, R.W. Gardner³⁷, N. Garelli¹⁵³, S. Gargiulo⁵², V. Garonne¹³⁴, A. Gaudiello^{55b,55a}, G. Gaudio^{70a}, I.L. Gavrilenko¹¹⁰, A. Gavrilyuk¹²³, C. Gay¹⁷⁵, G. Gaycken⁴⁶, E.N. Gazis¹⁰, A.A. Geanta^{27b}, C.M. Gee¹⁴⁶, C.N.P. Gee¹⁴⁴, J. Geisen⁵³, M. Geisen⁹⁹, C. Gemme^{55b}, M.H. Genest⁵⁸, C. Geng¹⁰⁵, S. Gentile^{72a,72b}, S. George⁹³, T. Geralis⁴⁴, L.O. Gerlach⁵³, P. Gessinger-Befurt⁹⁹, G. Gessner⁴⁷, S. Ghasemi¹⁵¹, M. Ghasemi Bostanabad¹⁷⁶, A. Ghosh¹³², A. Ghosh⁷⁷, B. Giacobbe^{23b}, S. Giagu^{72a,72b}, N. Giangiacomi^{23b,23a}, P. Giannetti^{71a}, A. Giannini^{69a,69b}, G. Giannini¹⁴, S.M. Gibson⁹³, M. Gignac¹⁴⁶, D. Gillberg³⁴, G. Gilles¹⁸², D.M. Gingrich^{3,ax}, M.P. Giordani^{66a,66c}, F.M. Giorgi^{23b}, P.F. Giraud¹⁴⁵, G. Giugliarelli^{66a,66c}, D. Giugni^{68a}, F. Giuliani^{73a,73b}, S. Gkaitatzis¹⁶², I. Gkialas^{9,h}, E.L. Gkoukousis¹⁴, P. Gkoutoumis¹⁰, L.K. Gladilin¹¹², C. Glasman⁹⁸, J. Glatzer¹⁴, P.C.F. Glaysheer⁴⁶, A. Glazov⁴⁶, G.R. Gledhill¹³¹, M. Goblirsch-Kolb²⁶, D. Godin¹⁰⁹, S. Goldfarb¹⁰⁴, T. Golling⁵⁴, D. Golubkov¹²², A. Gomes^{140a,140b}, R. Goncalves Gama⁵³, R. Gonçalves^{140a,140b}, G. Gonella⁵², L. Gonella²¹, A. Gongadze⁷⁹, F. Gonnella²¹, J.L. Gonski⁵⁹, S. González de la Hoz¹⁷⁴, S. Gonzalez-Sevilla⁵⁴, G.R. Gonzalvo Rodriguez¹⁷⁴, L. Goossens³⁶, P.A. Gorbounov¹²³, H.A. Gordon²⁹, B. Gorini³⁶,

E. Gorini ^{67a,67b}, A. Gorišek ⁹¹, A.T. Goshaw ⁴⁹, M.I. Gostkin ⁷⁹, C.A. Gottardo ¹¹⁸, M. Gouighri ^{35b}, D. Goujdam ^{35c}, A.G. Goussiou ¹⁴⁸, N. Govender ^{33b}, C. Goy ⁵, E. Gozani ¹⁶⁰, I. Grabowska-Bold ^{83a}, E.C. Graham ⁹⁰, J. Gramling ¹⁷¹, E. Gramstad ¹³⁴, S. Grancagnolo ¹⁹, M. Grandi ¹⁵⁶, V. Gratchev ¹³⁸, P.M. Gravila ^{27f}, F.G. Gravili ^{67a,67b}, C. Gray ⁵⁷, H.M. Gray ¹⁸, C. Grefe ²⁴, K. Gregersen ⁹⁶, I.M. Gregor ⁴⁶, P. Grenier ¹⁵³, K. Grevtsov ⁴⁶, C. Grieco ¹⁴, N.A. Grieser ¹²⁸, A.A. Grillo ¹⁴⁶, K. Grimm ^{31,l}, S. Grinstein ^{14,z}, J.-F. Grivaz ¹³², S. Groh ⁹⁹, E. Gross ¹⁸⁰, J. Grosse-Knetter ⁵³, Z.J. GROUT ⁹⁴, C. Grud ¹⁰⁵, A. Grummer ¹¹⁷, L. Guan ¹⁰⁵, W. Guan ¹⁸¹, J. Guenther ³⁶, A. Guerguichon ¹³², J.G.R. Guerrero Rojas ¹⁷⁴, F. Guescini ¹¹⁴, D. Guest ¹⁷¹, R. Gugel ⁹⁹, T. Guillemin ⁵, S. Guindon ³⁶, U. Gul ⁵⁷, J. Guo ^{60c}, W. Guo ¹⁰⁵, Y. Guo ^{60a,t}, Z. Guo ¹⁰¹, R. Gupta ⁴⁶, S. Gurbuz ^{12c}, G. Gustavino ¹²⁸, M. Guth ⁵², P. Gutierrez ¹²⁸, C. Gutschow ⁹⁴, C. Guyot ¹⁴⁵, C. Gwenlan ¹³⁵, C.B. Gwilliam ⁹⁰, A. Haas ¹²⁴, C. Haber ¹⁸, H.K. Hadavand ⁸, N. Haddad ^{35e}, A. Hadeef ^{60a}, S. Hageböck ³⁶, M. Haleem ¹⁷⁷, J. Haley ¹²⁹, G. Halladjian ¹⁰⁶, G.D. Hallowell ¹⁰¹, K. Hamacher ¹⁸², P. Hamal ¹³⁰, K. Hamano ¹⁷⁶, H. Hamdaoui ^{35e}, G.N. Hamity ¹⁴⁹, K. Han ^{60a,ak}, L. Han ^{60a}, S. Han ^{15a}, Y.F. Han ¹⁶⁷, K. Hanagaki ^{81,x}, M. Hance ¹⁴⁶, D.M. Handl ¹¹³, B. Haney ¹³⁷, R. Hankache ¹³⁶, E. Hansen ⁹⁶, J.B. Hansen ⁴⁰, J.D. Hansen ⁴⁰, M.C. Hansen ²⁴, P.H. Hansen ⁴⁰, E.C. Hanson ¹⁰⁰, K. Hara ¹⁶⁹, T. Harenberg ¹⁸², S. Harkusha ¹⁰⁷, P.F. Harrison ¹⁷⁸, N.M. Hartmann ¹¹³, Y. Hasegawa ¹⁵⁰, A. Hasib ⁵⁰, S. Hassani ¹⁴⁵, S. Haug ²⁰, R. Hauser ¹⁰⁶, L.B. Havener ³⁹, M. Havranek ¹⁴², C.M. Hawkes ²¹, R.J. Hawking ³⁶, D. Hayden ¹⁰⁶, C. Hayes ¹⁵⁵, R.L. Hayes ¹⁷⁵, C.P. Hays ¹³⁵, J.M. Hays ⁹², H.S. Hayward ⁹⁰, S.J. Haywood ¹⁴⁴, F. He ^{60a}, M.P. Heath ⁵⁰, V. Hedberg ⁹⁶, L. Heelan ⁸, S. Heer ²⁴, K.K. Heidegger ⁵², W.D. Heidorn ⁷⁸, J. Heilman ³⁴, S. Heim ⁴⁶, T. Heim ¹⁸, B. Heinemann ^{46,as}, J.J. Heinrich ¹³¹, L. Heinrich ³⁶, C. Heinz ⁵⁶, J. Hejbal ¹⁴¹, L. Helary ^{61b}, A. Held ¹⁷⁵, S. Hellesund ¹³⁴, C.M. Helling ¹⁴⁶, S. Hellman ^{45a,45b}, C. Helsens ³⁶, R.C.W. Henderson ⁸⁹, Y. Heng ¹⁸¹, S. Henkelmann ¹⁷⁵, A.M. Henriques Correia ³⁶, G.H. Herbert ¹⁹, H. Herde ²⁶, V. Herget ¹⁷⁷, Y. Hernández Jiménez ^{33d}, H. Herr ⁹⁹, M.G. Herrmann ¹¹³, T. Herrmann ⁴⁸, G. Herten ⁵², R. Hertenberger ¹¹³, L. Hervas ³⁶, T.C. Herwig ¹³⁷, G.G. Hesketh ⁹⁴, N.P. Hessey ^{168a}, A. Higashida ¹⁶³, S. Higashino ⁸¹, E. Higón-Rodríguez ¹⁷⁴, K. Hildebrand ³⁷, E. Hill ¹⁷⁶, J.C. Hill ³², K.K. Hill ²⁹, K.H. Hiller ⁴⁶, S.J. Hillier ²¹, M. Hils ⁴⁸, I. Hinchliffe ¹⁸, F. Hinterkeuser ²⁴, M. Hirose ¹³³, S. Hirose ⁵², D. Hirschbuehl ¹⁸², B. Hiti ⁹¹, O. Hladik ¹⁴¹, D.R. Hlaluku ^{33d}, X. Hoad ⁵⁰, J. Hobbs ¹⁵⁵, N. Hod ¹⁸⁰, M.C. Hodgkinson ¹⁴⁹, A. Hoecker ³⁶, F. Hoenig ¹¹³, D. Hohn ⁵², D. Hohov ¹³², T.R. Holmes ³⁷, M. Holzbock ¹¹³, L.B.A.H. Hommels ³², S. Honda ¹⁶⁹, T.M. Hong ¹³⁹, J.C. Honig ⁵², A. Hönle ¹¹⁴, B.H. Hooberman ¹⁷³, W.H. Hopkins ⁶, Y. Horii ¹¹⁶, P. Horn ⁴⁸, L.A. Horyn ³⁷, S. Hou ¹⁵⁸, A. Hoummada ^{35a}, J. Howarth ¹⁰⁰, J. Hoya ⁸⁸, M. Hrabovsky ¹³⁰, J. Hrdinka ⁷⁶, I. Hristova ¹⁹, J. Hrivnac ¹³², A. Hrynevich ¹⁰⁸, T. Hryn'ova ⁵, P.J. Hsu ⁶⁴, S.-C. Hsu ¹⁴⁸, Q. Hu ²⁹, S. Hu ^{60c}, Y.F. Hu ^{15a,15d}, D.P. Huang ⁹⁴, Y. Huang ^{60a}, Y. Huang ^{15a}, Z. Hubacek ¹⁴², F. Hubaut ¹⁰¹, M. Huebner ²⁴, F. Huegging ²⁴, T.B. Huffman ¹³⁵, M. Huhtinen ³⁶, R.F.H. Hunter ³⁴, P. Huo ¹⁵⁵, A.M. Hupe ³⁴, N. Huseynov ^{79,ag}, J. Huston ¹⁰⁶, J. Huth ⁵⁹, R. Hyneman ¹⁰⁵, S. Hyrych ^{28a}, G. Iacobucci ⁵⁴, G. Iakovidis ²⁹, I. Ibragimov ¹⁵¹, L. Iconomidou-Fayard ¹³², Z. Idrissi ^{35e}, P. Iengo ³⁶, R. Ignazzi ⁴⁰, O. Igonkina ^{119,ab,*}, R. Iguchi ¹⁶³, T. Iizawa ⁵⁴, Y. Ikegami ⁸¹, M. Ikeno ⁸¹, D. Iliadis ¹⁶², N. Ilic ^{118,167,ae}, F. Iltzsche ⁴⁸, G. Introzzi ^{70a,70b}, M. Iodice ^{74a}, K. Iordanidou ^{168a}, V. Ippolito ^{72a,72b}, M.F. Isacson ¹⁷², M. Ishino ¹⁶³, W. Islam ¹²⁹, C. Issever ^{19,46}, S. Istin ¹⁶⁰, F. Ito ¹⁶⁹, J.M. Iturbe Ponce ^{63a}, R. Iuppa ^{75a,75b}, A. Ivina ¹⁸⁰, H. Iwasaki ⁸¹, J.M. Izen ⁴³, V. Izzo ^{69a}, P. Jacka ¹⁴¹, P. Jackson ¹, R.M. Jacobs ²⁴, B.P. Jaeger ¹⁵², V. Jain ², G. Jäkel ¹⁸², K.B. Jakobi ⁹⁹, K. Jakobs ⁵², T. Jakoubek ¹⁴¹, J. Jamieson ⁵⁷, K.W. Janas ^{83a}, R. Jansky ⁵⁴, J. Janssen ²⁴, M. Janus ⁵³, P.A. Janus ^{83a}, G. Jarlskog ⁹⁶, N. Javadov ^{79,ag}, T. Javůrek ³⁶, M. Javurkova ⁵², F. Jeanneau ¹⁴⁵, L. Jeanty ¹³¹, J. Jejelava ^{159a,ah}, A. Jelinskas ¹⁷⁸, P. Jenni ^{52,b}, J. Jeong ⁴⁶, N. Jeong ⁴⁶, S. Jézéquel ⁵, H. Ji ¹⁸¹, J. Jia ¹⁵⁵, H. Jiang ⁷⁸, Y. Jiang ^{60a}, Z. Jiang ^{153,q}, S. Jiggins ⁵², F.A. Jimenez Morales ³⁸, J. Jimenez Pena ¹¹⁴, S. Jin ^{15c}, A. Jinaru ^{27b}, O. Jinnouchi ¹⁶⁵, H. Jivan ^{33d}, P. Johansson ¹⁴⁹, K.A. Johns ⁷, C.A. Johnson ⁶⁵, K. Jon-And ^{45a,45b}, R.W.L. Jones ⁸⁹, S.D. Jones ¹⁵⁶, S. Jones ⁷, T.J. Jones ⁹⁰, J. Jongmanns ^{61a}, P.M. Jorge ^{140a}, J. Jovicevic ³⁶, X. Ju ¹⁸, J.J. Jungbuerth ¹¹⁴, A. Juste Rozas ^{14,z}, A. Kaczmarska ⁸⁴, M. Kado ^{72a,72b}, H. Kagan ¹²⁶, M. Kagan ¹⁵³, A. Kahn ³⁹, C. Kahra ⁹⁹, T. Kaji ¹⁷⁹, E. Kajomovitz ¹⁶⁰, C.W. Kalderon ⁹⁶, A. Kaluza ⁹⁹, A. Kamenshchikov ¹²², M. Kaneda ¹⁶³, L. Kanjir ⁹¹, Y. Kano ¹¹⁶, V.A. Kantserov ¹¹¹, J. Kanzaki ⁸¹, L.S. Kaplan ¹⁸¹, D. Kar ^{33d}, K. Karava ¹³⁵, M.J. Kareem ^{168b}, S.N. Karpov ⁷⁹, Z.M. Karpova ⁷⁹, V. Kartvelishvili ⁸⁹, A.N. Karyukhin ¹²², L. Kashif ¹⁸¹, R.D. Kass ¹²⁶, A. Kastanas ^{45a,45b}, C. Kato ^{60d,60c}, J. Katzy ⁴⁶, K. Kawade ¹⁵⁰, K. Kawagoe ⁸⁷, T. Kawaguchi ¹¹⁶, T. Kawamoto ¹⁶³, G. Kawamura ⁵³, E.F. Kay ¹⁷⁶, V.F. Kazanin ^{121b,121a}, R. Keeler ¹⁷⁶, R. Kehoe ⁴², J.S. Keller ³⁴, E. Kellermann ⁹⁶, D. Kelsey ¹⁵⁶,

J.J. Kempster²¹, J. Kendrick²¹, K.E. Kennedy³⁹, O. Kepka¹⁴¹, S. Kersten¹⁸², B.P. Kerševan⁹¹, S. Ketabchi Haghighat¹⁶⁷, M. Khader¹⁷³, F. Khalil-Zada¹³, M. Khandoga¹⁴⁵, A. Khanov¹²⁹, A.G. Kharlamov^{121b,121a}, T. Kharlamova^{121b,121a}, E.E. Khoda¹⁷⁵, A. Khodinov¹⁶⁶, T.J. Khoo⁵⁴, E. Khramov⁷⁹, J. Khubua^{159b}, S. Kido⁸², M. Kiehn⁵⁴, C.R. Kilby⁹³, Y.K. Kim³⁷, N. Kimura⁹⁴, O.M. Kind¹⁹, B.T. King^{90,*}, D. Kirchmeier⁴⁸, J. Kirk¹⁴⁴, A.E. Kiryunin¹¹⁴, T. Kishimoto¹⁶³, D.P. Kisliuk¹⁶⁷, V. Kitali⁴⁶, O. Kivernyk⁵, T. Klapdor-Kleingrothaus⁵², M. Klassen^{61a}, M.H. Klein¹⁰⁵, M. Klein⁹⁰, U. Klein⁹⁰, K. Kleinknecht⁹⁹, P. Klimek¹²⁰, A. Klimentov²⁹, T. Klingl²⁴, T. Klioutchnikova³⁶, F.F. Klitzner¹¹³, P. Kluit¹¹⁹, S. Kluth¹¹⁴, E. Kneringer⁷⁶, E.B.F.G. Knoops¹⁰¹, A. Knue⁵², D. Kobayashi⁸⁷, T. Kobayashi¹⁶³, M. Kobel⁴⁸, M. Kocian¹⁵³, P. Kodys¹⁴³, P.T. Koenig²⁴, T. Koffas³⁴, N.M. Köhler³⁶, T. Koi¹⁵³, M. Kolb^{61b}, I. Koletsou⁵, T. Komarek¹³⁰, T. Kondo⁸¹, N. Kondrashova^{60c}, K. Köneke⁵², A.C. König¹¹⁸, T. Kono¹²⁵, R. Konoplich^{124,an}, V. Konstantinides⁹⁴, N. Konstantinidis⁹⁴, B. Konya⁹⁶, R. Kopeliansky⁶⁵, S. Koperny^{83a}, K. Korcyl⁸⁴, K. Kordas¹⁶², G. Koren¹⁶¹, A. Korn⁹⁴, I. Korolkov¹⁴, E.V. Korolkova¹⁴⁹, N. Korotkova¹¹², O. Kortner¹¹⁴, S. Kortner¹¹⁴, T. Kosek¹⁴³, V.V. Kostyukhin¹⁶⁶, A. Kotsokechagia¹³², A. Kotwal⁴⁹, A. Koulouris¹⁰, A. Kourkoulouli-Charalampidi^{70a,70b}, C. Kourkoulouli⁹, E. Kourlitis¹⁴⁹, V. Kouskoura²⁹, A.B. Kowalewska⁸⁴, R. Kowalewski¹⁷⁶, C. Kozakai¹⁶³, W. Kozanecki¹⁴⁵, A.S. Kozhin¹²², V.A. Kramarenko¹¹², G. Kramberger⁹¹, D. Krasnopevtsev^{60a}, M.W. Krasny¹³⁶, A. Krasznahorkay³⁶, D. Krauss¹¹⁴, J.A. Kremer^{83a}, J. Kretschmar⁹⁰, P. Krieger¹⁶⁷, F. Krieter¹¹³, A. Krishnan^{61b}, K. Krizka¹⁸, K. Kroeninger⁴⁷, H. Kroha¹¹⁴, J. Kroll¹⁴¹, J. Kroll¹³⁷, K.S. Krowpman¹⁰⁶, J. Krstic¹⁶, U. Kruchonak⁷⁹, H. Krüger²⁴, N. Krumnack⁷⁸, M.C. Kruse⁴⁹, J.A. Krzysiak⁸⁴, T. Kubota¹⁰⁴, O. Kuchinskaia¹⁶⁶, S. Kuday^{4b}, J.T. Kuechler⁴⁶, S. Kuehn³⁶, A. Kugel^{61a}, T. Kuhl⁴⁶, V. Kukhtin⁷⁹, R. Kukla¹⁰¹, Y. Kulchitsky^{107,aj}, S. Kuleshov^{147c}, Y.P. Kulinich¹⁷³, M. Kuna⁵⁸, T. Kunigo⁸⁵, A. Kupco¹⁴¹, T. Kupfer⁴⁷, O. Kuprash⁵², H. Kurashige⁸², L.L. Kurchaninov^{168a}, Y.A. Kurochkin¹⁰⁷, A. Kurova¹¹¹, M.G. Kurth^{15a,15d}, E.S. Kuwertz³⁶, M. Kuze¹⁶⁵, A.K. Kvam¹⁴⁸, J. Kvita¹³⁰, T. Kwan¹⁰³, A. La Rosa¹¹⁴, L. La Rotonda^{41b,41a}, F. La Ruffa^{41b,41a}, C. Lacasta¹⁷⁴, F. Lacava^{72a,72b}, D.P.J. Lack¹⁰⁰, H. Lacker¹⁹, D. Lacour¹³⁶, E. Ladygin⁷⁹, R. Lafaye⁵, B. Laforge¹³⁶, T. Lagouri^{33d}, S. Lai⁵³, S. Lammers⁶⁵, W. Lampl⁷, C. Lampoudis¹⁶², E. Lançon²⁹, U. Landgraf⁵², M.P.J. Landon⁹², M.C. Lanfermann⁵⁴, V.S. Lang⁴⁶, J.C. Lange⁵³, R.J. Langenberg³⁶, A.J. Lankford¹⁷¹, F. Lanni²⁹, K. Lantzscheid²⁴, A. Lanza^{70a}, A. Lapertosa^{55b,55a}, S. Laplace¹³⁶, J.F. Laporte¹⁴⁵, T. Lari^{68a}, F. Lasagni Manghi^{23b,23a}, M. Lassnig³⁶, T.S. Lau^{63a}, A. Laudrain¹³², A. Laurier³⁴, M. Lavorgna^{69a,69b}, S.D. Lawlor⁹³, M. Lazzaroni^{68a,68b}, B. Le¹⁰⁴, E. Le Guirriec¹⁰¹, M. LeBlanc⁷, T. LeCompte⁶, F. Ledroit-Guillon⁵⁸, A.C.A. Lee⁹⁴, C.A. Lee²⁹, G.R. Lee¹⁷, L. Lee⁵⁹, S.C. Lee¹⁵⁸, S.J. Lee³⁴, S. Lee⁷⁸, B. Lefebvre^{168a}, H.P. Lefebvre⁹³, M. Lefebvre¹⁷⁶, F. Legger¹¹³, C. Leggett¹⁸, K. Lehmann¹⁵², N. Lehmann¹⁸², G. Lehmann Miotto³⁶, W.A. Leight⁴⁶, A. Leisos^{162,y}, M.A.L. Leite^{80d}, C.E. Leitgeb¹¹³, R. Leitner¹⁴³, D. Lellouch^{180,*}, K.J.C. Leney⁴², T. Lenz²⁴, B. Lenzi³⁶, R. Leone⁷, S. Leone^{71a}, C. Leonidopoulos⁵⁰, A. Leopold¹³⁶, G. Lerner¹⁵⁶, C. Leroy¹⁰⁹, R. Les¹⁶⁷, C.G. Lester³², M. Levchenko¹³⁸, J. Levêque⁵, D. Levin¹⁰⁵, L.J. Levinson¹⁸⁰, D.J. Lewis²¹, B. Li^{15b}, B. Li¹⁰⁵, C.-Q. Li^{60a}, F. Li^{60c}, H. Li^{60a}, H. Li^{60b}, J. Li^{60c}, K. Li¹⁵³, L. Li^{60c}, M. Li^{15a,15d}, Q. Li^{15a,15d}, Q.Y. Li^{60a}, S. Li^{60d,60c}, X. Li⁴⁶, Y. Li⁴⁶, Z. Li^{60b}, Z. Liang^{15a}, B. Liberti^{73a}, A. Liblong¹⁶⁷, K. Lie^{63c}, C.Y. Lin³², K. Lin¹⁰⁶, T.H. Lin⁹⁹, R.A. Linck⁶⁵, J.H. Lindon²¹, A.L. Lioni⁵⁴, E. Lipeles¹³⁷, A. Lipniacka¹⁷, M. Lisovsky^{61b}, T.M. Liss^{173,au}, A. Lister¹⁷⁵, A.M. Litke¹⁴⁶, J.D. Little⁸, B. Liu⁷⁸, B.L. Liu²⁹, H.B. Liu¹⁰⁵, H. Liu¹⁰⁵, J.B. Liu^{60a}, J.K.K. Liu¹³⁵, K. Liu¹³⁶, M. Liu^{60a}, P. Liu¹⁸, Y. Liu^{15a,15d}, Y.L. Liu¹⁰⁵, Y.W. Liu^{60a}, M. Livan^{70a,70b}, A. Lleres⁵⁸, J. Llorente Merino¹⁵², S.L. Lloyd⁹², C.Y. Lo^{63b}, F. Lo Sterzo⁴², E.M. Lobodzinska⁴⁶, P. Loch⁷, S. Loffredo^{73a,73b}, T. Lohse¹⁹, K. Lohwasser¹⁴⁹, M. Lokajicek¹⁴¹, J.D. Long¹⁷³, R.E. Long⁸⁹, L. Longo³⁶, K.A. Looper¹²⁶, J.A. Lopez^{147c}, I. Lopez Paz¹⁰⁰, A. Lopez Solis¹⁴⁹, J. Lorenz¹¹³, N. Lorenzo Martinez⁵, M. Losada²², P.J. Lösel¹¹³, A. Lösle⁵², X. Lou⁴⁶, X. Lou^{15a}, A. Lounis¹³², J. Love⁶, P.A. Love⁸⁹, J.J. Lozano Bahilo¹⁷⁴, M. Lu^{60a}, Y.J. Lu⁶⁴, H.J. Lubatti¹⁴⁸, C. Luci^{72a,72b}, A. Lucotte⁵⁸, C. Luedtke⁵², F. Luehring⁶⁵, I. Luise¹³⁶, L. Luminari^{72a}, B. Lund-Jensen¹⁵⁴, M.S. Lutz¹⁰², D. Lynn²⁹, R. Lysak¹⁴¹, E. Lytken⁹⁶, F. Lyu^{15a}, V. Lyubushkin⁷⁹, T. Lyubushkina⁷⁹, H. Ma²⁹, L.L. Ma^{60b}, Y. Ma^{60b}, G. Maccarrone⁵¹, A. Macchiolo¹¹⁴, C.M. Macdonald¹⁴⁹, J. Machado Miguens¹³⁷, D. Madaffari¹⁷⁴, R. Madar³⁸, W.F. Mader⁴⁸, N. Madysa⁴⁸, J. Maeda⁸², T. Maeno²⁹, M. Maerker⁴⁸, A.S. Maevskiy¹¹², V. Magerl⁵², N. Magini⁷⁸, D.J. Mahon³⁹, C. Maidantchik^{80b}, T. Maier¹¹³, A. Maio^{140a,140b,140d}, K. Maj^{83a}, O. Majersky^{28a}, S. Majewski¹³¹, Y. Makida⁸¹, N. Makovec¹³², B. Malaescu¹³⁶, Pa. Malecki⁸⁴, V.P. Maleev¹³⁸, F. Malek⁵⁸, U. Mallik⁷⁷, D. Malon⁶, C. Malone³², S. Maltezos¹⁰, S. Malyukov⁷⁹,

J. Mamuzic¹⁷⁴, G. Mancini⁵¹, I. Mandić⁹¹, L. Manhaes de Andrade Filho^{80a}, I.M. Maniatis¹⁶²,
J. Manjarres Ramos⁴⁸, K.H. Mankinen⁹⁶, A. Mann¹¹³, A. Manousos⁷⁶, B. Mansoulie¹⁴⁵, I. Manthos¹⁶²,
S. Manzoni¹¹⁹, A. Marantis¹⁶², G. Marceca³⁰, L. Marchese¹³⁵, G. Marchiori¹³⁶, M. Marcisovsky¹⁴¹,
L. Maroccia^{73a,73b}, C. Marcon⁹⁶, C.A. Marin Tobon³⁶, M. Marjanovic¹²⁸, Z. Marshall¹⁸,
M.U.F. Martensson¹⁷², S. Marti-Garcia¹⁷⁴, C.B. Martin¹²⁶, T.A. Martin¹⁷⁸, V.J. Martin⁵⁰,
B. Martin dit Latour¹⁷, L. Martinelli^{74a,74b}, M. Martinez^{14,z}, V.I. Martinez Outschoorn¹⁰²,
S. Martin-Haugh¹⁴⁴, V.S. Martoiu^{27b}, A.C. Martyniuk⁹⁴, A. Marzin³⁶, S.R. Maschek¹¹⁴, L. Masetti⁹⁹,
T. Mashimo¹⁶³, R. Mashinistov¹¹⁰, J. Masik¹⁰⁰, A.L. Maslennikov^{121b,121a}, L. Massa^{73a,73b},
P. Massarotti^{69a,69b}, P. Mastrandrea^{71a,71b}, A. Mastroberardino^{41b,41a}, T. Masubuchi¹⁶³, D. Matakias¹⁰,
A. Matic¹¹³, P. Mättig²⁴, J. Maurer^{27b}, B. Maček⁹¹, D.A. Maximov^{121b,121a}, R. Mazini¹⁵⁸, I. Maznas¹⁶²,
S.M. Mazza¹⁴⁶, S.P. Mc Kee¹⁰⁵, T.G. McCarthy¹¹⁴, W.P. McCormack¹⁸, E.F. McDonald¹⁰⁴, J.A. Mcfayden³⁶,
G. Mchedlidze^{159b}, M.A. McKay⁴², K.D. McLean¹⁷⁶, S.J. McMahon¹⁴⁴, P.C. McNamara¹⁰⁴, C.J. McNicol¹⁷⁸,
R.A. McPherson^{176,ae}, J.E. Mdhuli^{33d}, Z.A. Meadows¹⁰², S. Meehan³⁶, T. Megy⁵², S. Mehlhase¹¹³,
A. Mehta⁹⁰, T. Meideck⁵⁸, B. Meirose⁴³, D. Melini¹⁷⁴, B.R. Mellado Garcia^{33d}, J.D. Mellenthin⁵³,
M. Melo^{28a}, F. Meloni⁴⁶, A. Melzer²⁴, S.B. Menary¹⁰⁰, E.D. Mendes Gouveia^{140a,140e}, L. Meng³⁶,
X.T. Meng¹⁰⁵, S. Menke¹¹⁴, E. Meoni^{41b,41a}, S. Mergelmeyer¹⁹, S.A.M. Merkt¹³⁹, C. Merlassino²⁰,
P. Mermod⁵⁴, L. Merola^{69a,69b}, C. Meroni^{68a}, O. Meshkov^{112,110}, J.K.R. Meshreki¹⁵¹, A. Messina^{72a,72b},
J. Metcalfe⁶, A.S. Mete¹⁷¹, C. Meyer⁶⁵, J. Meyer¹⁶⁰, J.-P. Meyer¹⁴⁵, H. Meyer Zu Theenhausen^{61a},
F. Miano¹⁵⁶, M. Michetti¹⁹, R.P. Middleton¹⁴⁴, L. Mijović⁵⁰, G. Mikenberg¹⁸⁰, M. Mikestikova¹⁴¹,
M. Mikuž⁹¹, H. Mildner¹⁴⁹, M. Milesi¹⁰⁴, A. Milic¹⁶⁷, D.A. Millar⁹², D.W. Miller³⁷, A. Milov¹⁸⁰,
D.A. Milstead^{45a,45b}, R.A. Mina^{153,q}, A.A. Minaenko¹²², M. Miñano Moya¹⁷⁴, I.A. Minashvili^{159b},
A.I. Mincer¹²⁴, B. Mindur^{83a}, M. Mineev⁷⁹, Y. Minegishi¹⁶³, L.M. Mir¹⁴, A. Mirto^{67a,67b}, K.P. Mistry¹³⁷,
T. Mitani¹⁷⁹, J. Mitrevski¹¹³, V.A. Mitsou¹⁷⁴, M. Mittal^{60c}, O. Miu¹⁶⁷, A. Miucci²⁰, P.S. Miyagawa¹⁴⁹,
A. Mizukami⁸¹, J.U. Mjörnmark⁹⁶, T. Mkrtchyan¹⁸⁴, M. Mlynarikova¹⁴³, T. Moa^{45a,45b}, K. Mochizuki¹⁰⁹,
P. Mogg⁵², S. Mohapatra³⁹, R. Moles-Valls²⁴, M.C. Mondragon¹⁰⁶, K. Mönig⁴⁶, J. Monk⁴⁰,
E. Monnier¹⁰¹, A. Montalbano¹⁵², J. Montejo Berlingen³⁶, M. Montella⁹⁴, F. Monticelli⁸⁸, S. Monzani^{68a},
N. Morange¹³², D. Moreno²², M. Moreno Llácer¹⁷⁴, C. Moreno Martinez¹⁴, P. Morettini^{55b},
M. Morgenstern¹¹⁹, S. Morgenstern⁴⁸, D. Mori¹⁵², M. Morii⁵⁹, M. Morinaga¹⁷⁹, V. Morisbak¹³⁴,
A.K. Morley³⁶, G. Mornacchi³⁶, A.P. Morris⁹⁴, L. Morvaj¹⁵⁵, P. Moschovakos³⁶, B. Moser¹¹⁹,
M. Mosidze^{159b}, T. Moskalets¹⁴⁵, H.J. Moss¹⁴⁹, J. Moss^{31,n}, E.J.W. Moyse¹⁰², S. Muanza¹⁰¹, J. Mueller¹³⁹,
R.S.P. Mueller¹¹³, D. Muenstermann⁸⁹, G.A. Mullier⁹⁶, D.P. Mungo^{68a,68b}, J.L. Munoz Martinez¹⁴,
F.J. Munoz Sanchez¹⁰⁰, P. Murin^{28b}, W.J. Murray^{178,144}, A. Murrone^{68a,68b}, M. Muškinja¹⁸,
C. Mwewa^{33a}, A.G. Myagkov^{122,ao}, J. Myers¹³¹, M. Myska¹⁴², B.P. Nachman¹⁸, O. Nackenhorst⁴⁷,
A. Nag Nag⁴⁸, K. Nagai¹³⁵, K. Nagano⁸¹, Y. Nagasaka⁶², M. Nagel⁵², J.L. Nagle²⁹, E. Nagy¹⁰¹,
A.M. Nairz³⁶, Y. Nakahama¹¹⁶, K. Nakamura⁸¹, T. Nakamura¹⁶³, I. Nakano¹²⁷, H. Nanjo¹³³,
F. Napolitano^{61a}, R.F. Naranjo Garcia⁴⁶, R. Narayan⁴², I. Naryshkin¹³⁸, T. Naumann⁴⁶, G. Navarro²²,
P.Y. Nechaeva¹¹⁰, F. Nechansky⁴⁶, T.J. Neep²¹, A. Negri^{70a,70b}, M. Negrini^{23b}, C. Nellist⁵³,
M.E. Nelson¹³⁵, S. Nemecek¹⁴¹, P. Nemethy¹²⁴, M. Nessi^{36,d}, M.S. Neubauer¹⁷³, M. Neumann¹⁸²,
P.R. Newman²¹, Y.S. Ng¹⁹, Y.W.Y. Ng¹⁷¹, B. Ngair^{35e}, H.D.N. Nguyen¹⁰¹, T. Nguyen Manh¹⁰⁹,
E. Nibigira³⁸, R.B. Nickerson¹³⁵, R. Nicolaïdou¹⁴⁵, D.S. Nielsen⁴⁰, J. Nielsen¹⁴⁶, N. Nikiforou¹¹,
V. Nikolaenko^{122,ao}, I. Nikolic-Audit¹³⁶, K. Nikolopoulos²¹, P. Nilsson²⁹, H.R. Nindhito⁵⁴, Y. Ninomiya⁸¹,
A. Nisati^{72a}, N. Nishu^{60c}, R. Nisius¹¹⁴, I. Nitsche⁴⁷, T. Nitta¹⁷⁹, T. Nobe¹⁶³, Y. Noguchi⁸⁵, I. Nomidis¹³⁶,
M.A. Nomura²⁹, M. Nordberg³⁶, N. Norjoharuddeen¹³⁵, T. Novak⁹¹, O. Novgorodova⁴⁸, R. Novotny¹⁴²,
L. Nozka¹³⁰, K. Ntekas¹⁷¹, E. Nurse⁹⁴, F.G. Oakham^{34,ax}, H. Oberlack¹¹⁴, J. Ocariz¹³⁶, A. Ochi⁸²,
I. Ochoa³⁹, J.P. Ochoa-Ricoux^{147a}, K. O'Connor²⁶, S. Oda⁸⁷, S. Odaka⁸¹, S. Oerdek⁵³, A. Ogrodnik^{83a},
A. Oh¹⁰⁰, S.H. Oh⁴⁹, C.C. Ohm¹⁵⁴, H. Oide¹⁶⁵, M.L. Ojeda¹⁶⁷, H. Okawa¹⁶⁹, Y. Okazaki⁸⁵,
Y. Okumura¹⁶³, T. Okuyama⁸¹, A. Olariu^{27b}, L.F. Oleiro Seabra^{140a}, S.A. Olivares Pino^{147a},
D. Oliveira Damazio²⁹, J.L. Oliver¹, M.J.R. Olsson¹⁷¹, A. Olszewski⁸⁴, J. Olszowska⁸⁴, D.C. O'Neil¹⁵²,
A.P. O'Neill¹³⁵, A. Onofre^{140a,140e}, P.U.E. Onyisi¹¹, H. Oppen¹³⁴, M.J. Oreglia³⁷, G.E. Orellana⁸⁸,
D. Orestano^{74a,74b}, N. Orlando¹⁴, R.S. Orr¹⁶⁷, V. O'Shea⁵⁷, R. Ospanov^{60a}, G. Otero y Garzon³⁰,
H. Otono⁸⁷, P.S. Ott^{61a}, M. Ouchrif^{35d}, J. Ouellette²⁹, F. Ould-Saada¹³⁴, A. Ouraou¹⁴⁵, Q. Ouyang^{15a},
M. Owen⁵⁷, R.E. Owen²¹, V.E. Ozcan^{12c}, N. Ozturk⁸, J. Pacalt¹³⁰, H.A. Pacey³², K. Pachal⁴⁹,

A. Pacheco Pages¹⁴, C. Padilla Aranda¹⁴, S. Pagan Griso¹⁸, M. Paganini¹⁸³, G. Palacino⁶⁵, S. Palazzo⁵⁰, S. Palestini³⁶, M. Palka^{83b}, D. Pallin³⁸, I. Panagoulas¹⁰, C.E. Pandini³⁶, J.G. Panduro Vazquez⁹³, P. Pani⁴⁶, G. Panizzo^{66a,66c}, L. Paolozzi⁵⁴, C. Papadatos¹⁰⁹, K. Papageorgiou^{9,h}, S. Parajuli⁴³, A. Paramonov⁶, D. Paredes Hernandez^{63b}, S.R. Paredes Saenz¹³⁵, B. Parida¹⁶⁶, T.H. Park¹⁶⁷, A.J. Parker³¹, M.A. Parker³², F. Parodi^{55b,55a}, E.W. Parrish¹²⁰, J.A. Parsons³⁹, U. Parzefall⁵², L. Pascual Dominguez¹³⁶, V.R. Pascuzzi¹⁶⁷, J.M.P. Pasner¹⁴⁶, F. Pasquali¹¹⁹, E. Pasqualucci^{72a}, S. Passaggio^{55b}, F. Pastore⁹³, P. Pasuwan^{45a,45b}, S. Patariaia⁹⁹, J.R. Pater¹⁰⁰, A. Pathak^{181,j}, T. Pauly³⁶, B. Pearson¹¹⁴, M. Pedersen¹³⁴, L. Pedraza Diaz¹¹⁸, R. Pedro^{140a}, T. Peiffer⁵³, S.V. Peleganchuk^{121b,121a}, O. Penc¹⁴¹, H. Peng^{60a}, B.S. Peralva^{80a}, M.M. Perego¹³², A.P. Pereira Peixoto^{140a}, D.V. Perepelitsa²⁹, F. Peri¹⁹, L. Perini^{68a,68b}, H. Pernegger³⁶, S. Perrella^{69a,69b}, K. Peters⁴⁶, R.F.Y. Peters¹⁰⁰, B.A. Petersen³⁶, T.C. Petersen⁴⁰, E. Petit¹⁰¹, A. Petridis¹, C. Petridou¹⁶², P. Petroff¹³², M. Petrov¹³⁵, F. Petrucci^{74a,74b}, M. Pettee¹⁸³, N.E. Pettersson¹⁰², K. Petukhova¹⁴³, A. Peyaud¹⁴⁵, R. Pezoa^{147c}, L. Pezzotti^{70a,70b}, T. Pham¹⁰⁴, F.H. Phillips¹⁰⁶, P.W. Phillips¹⁴⁴, M.W. Phipps¹⁷³, G. Piacquadio¹⁵⁵, E. Pianori¹⁸, A. Picazio¹⁰², R.H. Pickles¹⁰⁰, R. Piegaiia³⁰, D. Pietreanu^{27b}, J.E. Pilcher³⁷, A.D. Pilkington¹⁰⁰, M. Pinamonti^{73a,73b}, J.L. Pinfold³, M. Pitt¹⁶¹, L. Pizzimento^{73a,73b}, M.-A. Pleier²⁹, V. Pleskot¹⁴³, E. Plotnikova⁷⁹, P. Podberezko^{121b,121a}, R. Poettgen⁹⁶, R. Poggi⁵⁴, L. Poggioli¹³², I. Pogrebnyak¹⁰⁶, D. Pohl²⁴, I. Pokharel⁵³, G. Polesello^{70a}, A. Poley¹⁸, A. Policicchio^{72a,72b}, R. Polifka¹⁴³, A. Polini^{23b}, C.S. Pollard⁴⁶, V. Polychronakos²⁹, D. Ponomarenko¹¹¹, L. Pontecorvo³⁶, S. Popa^{27a}, G.A. Popeneciu^{27d}, L. Portales⁵, D.M. Portillo Quintero⁵⁸, S. Pospisil¹⁴², K. Potamianos⁴⁶, I.N. Potrap⁷⁹, C.J. Potter³², H. Potti¹¹, T. Poulsen⁹⁶, J. Poveda³⁶, T.D. Powell¹⁴⁹, G. Pownall⁴⁶, M.E. Pozo Astigarraga³⁶, P. Pralavorio¹⁰¹, S. Prell⁷⁸, D. Price¹⁰⁰, M. Primavera^{67a}, S. Prince¹⁰³, M.L. Proffitt¹⁴⁸, N. Proklova¹¹¹, K. Prokofiev^{63c}, F. Prokoshin⁷⁹, S. Protopopescu²⁹, J. Proudfoot⁶, M. Przybycien^{83a}, D. Pudzha¹³⁸, A. Puri¹⁷³, P. Puzo¹³², J. Qian¹⁰⁵, Y. Qin¹⁰⁰, A. Quadt⁵³, M. Queitsch-Maitland⁴⁶, A. Qureshi¹, M. Racko^{28a}, P. Rados¹⁰⁴, F. Ragusa^{68a,68b}, G. Rahal⁹⁷, J.A. Raine⁵⁴, S. Rajagopalan²⁹, A. Ramirez Morales⁹², K. Ran^{15a,15d}, T. Rashid¹³², S. Raspopov⁵, D.M. Rauch⁴⁶, F. Rauscher¹¹³, S. Rave⁹⁹, B. Ravina¹⁴⁹, I. Ravinovich¹⁸⁰, J.H. Rawling¹⁰⁰, M. Raymond³⁶, A.L. Read¹³⁴, N.P. Readioff⁵⁸, M. Reale^{67a,67b}, D.M. Rebuzzi^{70a,70b}, A. Redelbach¹⁷⁷, G. Redlinger²⁹, K. Reeves⁴³, L. Rehnisch¹⁹, J. Reichert¹³⁷, D. Reikher¹⁶¹, A. Reiss⁹⁹, A. Rej¹⁵¹, C. Rembser³⁶, M. Renda^{27b}, M. Rescigno^{72a}, S. Resconi^{68a}, E.D. Resseguie¹³⁷, S. Rettie¹⁷⁵, E. Reynolds²¹, O.L. Rezanova^{121b,121a}, P. Reznicek¹⁴³, E. Ricci^{75a,75b}, R. Richter¹¹⁴, S. Richter⁴⁶, E. Richter-Was^{83b}, O. Ricken²⁴, M. Ridel¹³⁶, P. Rieck¹¹⁴, O. Rifki⁴⁶, M. Rijssenbeek¹⁵⁵, A. Rimoldi^{70a,70b}, M. Rimoldi⁴⁶, L. Rinaldi^{23b}, G. Ripellino¹⁵⁴, I. Riu¹⁴, J.C. Rivera Vergara¹⁷⁶, F. Rizatdinova¹²⁹, E. Rizvi⁹², C. Rizzi³⁶, R.T. Roberts¹⁰⁰, S.H. Robertson^{103,ae}, M. Robin⁴⁶, D. Robinson³², J.E.M. Robinson⁴⁶, C.M. Robles Gajardo^{147c}, A. Robson⁵⁷, A. Rocchi^{73a,73b}, E. Rocco⁹⁹, C. Roda^{71a,71b}, S. Rodriguez Bosca¹⁷⁴, A. Rodriguez Perez¹⁴, D. Rodriguez Rodriguez¹⁷⁴, A.M. Rodríguez Vera^{168b}, S. Roe³⁶, O. Röhne¹³⁴, R. Röhrig¹¹⁴, R.A. Rojas^{147c}, C.P.A. Roland⁶⁵, J. Roloff²⁹, A. Romaniouk¹¹¹, M. Romano^{23b,23a}, N. Rompotis⁹⁰, M. Ronzani¹²⁴, L. Roos¹³⁶, S. Rosati^{72a}, K. Rosbach⁵², G. Rosin¹⁰², B.J. Rosser¹³⁷, E. Rossi⁴⁶, E. Rossi^{74a,74b}, E. Rossi^{69a,69b}, L.P. Rossi^{55b}, L. Rossini^{68a,68b}, R. Rosten¹⁴, M. Rotaru^{27b}, J. Rothberg¹⁴⁸, D. Rousseau¹³², G. Rovelli^{70a,70b}, A. Roy¹¹, D. Roy^{33d}, A. Rozanov¹⁰¹, Y. Rozen¹⁶⁰, X. Ruan^{33d}, F. Rühr⁵², A. Ruiz-Martinez¹⁷⁴, A. Rummler³⁶, Z. Rurikova⁵², N.A. Rusakovich⁷⁹, H.L. Russell¹⁰³, L. Rustige^{38,47}, J.P. Rutherford⁷, E.M. Rüttinger¹⁴⁹, M. Rybar³⁹, G. Rybkin¹³², E.B. Rye¹³⁴, A. Ryzhov¹²², P. Sabatini⁵³, G. Sabato¹¹⁹, S. Sacerdoti¹³², H.F.-W. Sadrozinski¹⁴⁶, R. Sadykov⁷⁹, F. Safai Tehrani^{72a}, B. Safarzadeh Samani¹⁵⁶, P. Saha¹²⁰, S. Saha¹⁰³, M. Sahinsoy^{61a}, A. Sahu¹⁸², M. Saimpert⁴⁶, M. Saito¹⁶³, T. Saito¹⁶³, H. Sakamoto¹⁶³, A. Sakharov^{124,an}, D. Salamani⁵⁴, G. Salamanna^{74a,74b}, J.E. Salazar Loyola^{147c}, A. Salnikov¹⁵³, J. Salt¹⁷⁴, D. Salvatore^{41b,41a}, F. Salvatore¹⁵⁶, A. Salvucci^{63a,63b,63c}, A. Salzburger³⁶, J. Samarati³⁶, D. Sammel⁵², D. Sampsonidis¹⁶², D. Sampsonidou¹⁶², J. Sánchez¹⁷⁴, A. Sanchez Pineda^{66a,66c}, H. Sandaker¹³⁴, C.O. Sander⁴⁶, I.G. Sanderswood⁸⁹, M. Sandhoff¹⁸², C. Sandoval²², D.P.C. Sankey¹⁴⁴, M. Sannino^{55b,55a}, Y. Sano¹¹⁶, A. Sansoni⁵¹, C. Santoni³⁸, H. Santos^{140a,140b}, S.N. Santpur¹⁸, A. Santra¹⁷⁴, A. Saprionov⁷⁹, J.G. Saraiva^{140a,140d}, O. Sasaki⁸¹, K. Sato¹⁶⁹, F. Sauerburger⁵², E. Sauvan⁵, P. Savard^{167,ax}, N. Savic¹¹⁴, R. Sawada¹⁶³, C. Sawyer¹⁴⁴, L. Sawyer^{95,al}, C. Sbarra^{23b}, A. Sbrizzi^{23a}, T. Scanlon⁹⁴, J. Schaarschmidt¹⁴⁸, P. Schacht¹¹⁴, B.M. Schachtner¹¹³, D. Schaefer³⁷, L. Schaefer¹³⁷, J. Schaeffer⁹⁹, S. Schaepe³⁶, U. Schäfer⁹⁹, A.C. Schaffer¹³², D. Schaile¹¹³, R.D. Schamberger¹⁵⁵, N. Scharmberg¹⁰⁰,

V.A. Schegelsky¹³⁸, D. Scheirich¹⁴³, F. Schenck¹⁹, M. Schernau¹⁷¹, C. Schiavi^{55b,55a}, S. Schier¹⁴⁶, L.K. Schildgen²⁴, Z.M. Schillaci²⁶, E.J. Schioppa³⁶, M. Schioppa^{41b,41a}, K.E. Schleicher⁵², S. Schlenker³⁶, K.R. Schmidt-Sommerfeld¹¹⁴, K. Schmieden³⁶, C. Schmitt⁹⁹, S. Schmitt⁴⁶, S. Schmitz⁹⁹, J.C. Schmoeckel⁴⁶, U. Schnoor⁵², L. Schoeffel¹⁴⁵, A. Schoening^{61b}, P.G. Scholer⁵², E. Schopf¹³⁵, M. Schott⁹⁹, J.F.P. Schouwenger¹¹⁸, J. Schovancova³⁶, S. Schramm⁵⁴, F. Schroeder¹⁸², A. Schulte⁹⁹, H.-C. Schultz-Coulon^{61a}, M. Schumacher⁵², B.A. Schumm¹⁴⁶, Ph. Schune¹⁴⁵, A. Schwartzman¹⁵³, T.A. Schwarz¹⁰⁵, Ph. Schwemling¹⁴⁵, R. Schwienhorst¹⁰⁶, A. Sciandra¹⁴⁶, G. Sciolla²⁶, M. Scodeggio⁴⁶, M. Scornajenghi^{41b,41a}, F. Scuri^{71a}, F. Scutti¹⁰⁴, L.M. Scyboz¹¹⁴, C.D. Sebastiani^{72a,72b}, P. Seema¹⁹, S.C. Seidel¹¹⁷, A. Seiden¹⁴⁶, B.D. Seidlitz²⁹, T. Seiss³⁷, J.M. Seixas^{80b}, G. Sekhniaidze^{69a}, K. Sekhon¹⁰⁵, S.J. Sekula⁴², N. Semprini-Cesari^{23b,23a}, S. Sen⁴⁹, C. Serfon⁷⁶, L. Serin¹³², L. Serkin^{66a,66b}, M. Sessa^{60a}, H. Severini¹²⁸, T. Šfiligoj⁹¹, F. Sforza^{55b,55a}, A. Sfyrla⁵⁴, E. Shabalina⁵³, J.D. Shahinian¹⁴⁶, N.W. Shaikh^{45a,45b}, D. Shaked Renous¹⁸⁰, L.Y. Shan^{15a}, J.T. Shank²⁵, M. Shapiro¹⁸, A. Sharma¹³⁵, A.S. Sharma¹, P.B. Shatalov¹²³, K. Shaw¹⁵⁶, S.M. Shaw¹⁰⁰, A. Shcherbakova¹³⁸, M. Shehade¹⁸⁰, Y. Shen¹²⁸, N. Sherafati³⁴, A.D. Sherman²⁵, P. Sherwood⁹⁴, L. Shi^{158,at}, S. Shimizu⁸¹, C.O. Shimmin¹⁸³, Y. Shimogama¹⁷⁹, M. Shimojima¹¹⁵, I.P.J. Shipsey¹³⁵, S. Shirabe⁸⁷, M. Shiyakova^{79,ac}, J. Shlomi¹⁸⁰, A. Shmeleva¹¹⁰, M.J. Shochet³⁷, J. Shojaii¹⁰⁴, D.R. Shope¹²⁸, S. Shrestha¹²⁶, E.M. Shrif^{33d}, E. Shulga¹⁸⁰, P. Sicho¹⁴¹, A.M. Sickles¹⁷³, P.E. Sidebo¹⁵⁴, E. Sideras Haddad^{33d}, O. Sidiropoulou³⁶, A. Sidoti^{23b,23a}, F. Siegert⁴⁸, Dj. Sijacki¹⁶, M.Jr. Silva¹⁸¹, M.V. Silva Oliveira^{80a}, S.B. Silverstein^{45a}, S. Simion¹³², E. Simioni⁹⁹, R. Simoniello⁹⁹, S. Simsek^{12b}, P. Sinervo¹⁶⁷, V. Sinetckii^{112,110}, N.B. Sinev¹³¹, M. Sioli^{23b,23a}, I. Siral¹⁰⁵, S.Yu. Sivoklov¹¹², J. Sjölin^{45a,45b}, E. Skorda⁹⁶, P. Skubic¹²⁸, M. Slawinska⁸⁴, K. Sliwa¹⁷⁰, R. Slovak¹⁴³, V. Smakhtin¹⁸⁰, B.H. Smart¹⁴⁴, J. Smiesko^{28a}, N. Smirnov¹¹¹, S.Yu. Smirnov¹¹¹, Y. Smirnov¹¹¹, L.N. Smirnova^{112,v}, O. Smirnova⁹⁶, J.W. Smith⁵³, M. Smizanska⁸⁹, K. Smolek¹⁴², A. Smykiewicz⁸⁴, A.A. Snesarev¹¹⁰, H.L. Snoek¹¹⁹, I.M. Snyder¹³¹, S. Snyder²⁹, R. Sobie^{176,ae}, A. Soffer¹⁶¹, A. Søgaard⁵⁰, F. Sohns⁵³, C.A. Solans Sanchez³⁶, E.Yu. Soldatov¹¹¹, U. Soldevila¹⁷⁴, A.A. Solodkov¹²², A. Soloshenko⁷⁹, O.V. Solovyanov¹²², V. Solovyev¹³⁸, P. Sommer¹⁴⁹, H. Son¹⁷⁰, W. Song¹⁴⁴, W.Y. Song^{168b}, A. Sopczak¹⁴², F. Sopkova^{28b}, C.L. Sotiropoulou^{71a,71b}, S. Sottocornola^{70a,70b}, R. Soualah^{66a,66c,g}, A.M. Soukharev^{121b,121a}, D. South⁴⁶, S. Spagnolo^{67a,67b}, M. Spalla¹¹⁴, M. Spangenberg¹⁷⁸, F. Spanò⁹³, D. Sperlich⁵², T.M. Spieker^{61a}, R. Spighi^{23b}, G. Spigo³⁶, M. Spina¹⁵⁶, D.P. Spiteri⁵⁷, M. Spousta¹⁴³, A. Stabile^{68a,68b}, B.L. Stamas¹²⁰, R. Stamen^{61a}, M. Stamenkovic¹¹⁹, E. Stanecka⁸⁴, B. Stanislaus¹³⁵, M.M. Stanitzki⁴⁶, M. Stankaityte¹³⁵, B. Stapf¹¹⁹, E.A. Starchenko¹²², G.H. Stark¹⁴⁶, J. Stark⁵⁸, S.H. Stark⁴⁰, P. Staroba¹⁴¹, P. Starovoitov^{61a}, S. Stärz¹⁰³, R. Staszewski⁸⁴, G. Stavropoulos⁴⁴, M. Stegler⁴⁶, P. Steinberg²⁹, A.L. Steinhebel¹³¹, B. Stelzer¹⁵², H.J. Stelzer¹³⁹, O. Stelzer-Chilton^{168a}, H. Stenzel⁵⁶, T.J. Stevenson¹⁵⁶, G.A. Stewart³⁶, M.C. Stockton³⁶, G. Stoicea^{27b}, M. Stolarski^{140a}, S. Stonjek¹¹⁴, A. Straessner⁴⁸, J. Strandberg¹⁵⁴, S. Strandberg^{45a,45b}, M. Strauss¹²⁸, P. Strizenec^{28b}, R. Ströhmer¹⁷⁷, D.M. Strom¹³¹, R. Stroynowski⁴², A. Strubig⁵⁰, S.A. Stucci²⁹, B. Stugu¹⁷, J. Stupak¹²⁸, N.A. Styles⁴⁶, D. Su¹⁵³, S. Suchek^{61a}, V.V. Sulin¹¹⁰, M.J. Sullivan⁹⁰, D.M.S. Sultan⁵⁴, S. Sultansoy^{4c}, T. Sumida⁸⁵, S. Sun¹⁰⁵, X. Sun³, K. Suruliz¹⁵⁶, C.J.E. Suster¹⁵⁷, M.R. Sutton¹⁵⁶, S. Suzuki⁸¹, M. Svatos¹⁴¹, M. Swiatlowski³⁷, S.P. Swift², T. Swirski¹⁷⁷, A. Sydorenko⁹⁹, I. Sykora^{28a}, M. Sykora¹⁴³, T. Sykora¹⁴³, D. Ta⁹⁹, K. Tackmann^{46,aa}, J. Taenzer¹⁶¹, A. Taffard¹⁷¹, R. Tahirout^{168a}, H. Takai²⁹, R. Takashima⁸⁶, K. Takeda⁸², T. Takeshita¹⁵⁰, E.P. Takeva⁵⁰, Y. Takubo⁸¹, M. Talby¹⁰¹, A.A. Talyshev^{121b,121a}, N.M. Tamir¹⁶¹, J. Tanaka¹⁶³, M. Tanaka¹⁶⁵, R. Tanaka¹³², S. Tapia Araya¹⁷³, S. Tapprogge⁹⁹, A. Tarek Abouelfadl Mohamed¹³⁶, S. Tarem¹⁶⁰, K. Tariq^{60b}, G. Tarna^{27b,c}, G.F. Tartarelli^{68a}, P. Tas¹⁴³, M. Tasevsky¹⁴¹, T. Tashiro⁸⁵, E. Tassi^{41b,41a}, A. Tavares Delgado^{140a,140b}, Y. Tayalati^{35e}, A.J. Taylor⁵⁰, G.N. Taylor¹⁰⁴, W. Taylor^{168b}, A.S. Tee⁸⁹, R. Teixeira De Lima¹⁵³, P. Teixeira-Dias⁹³, H. Ten Kate³⁶, J.J. Teoh¹¹⁹, S. Terada⁸¹, K. Terashi¹⁶³, J. Terron⁹⁸, S. Terzo¹⁴, M. Testa⁵¹, R.J. Teuscher^{167,ae}, S.J. Thais¹⁸³, T. Theveneaux-Pelzer⁴⁶, F. Thiele⁴⁰, D.W. Thomas⁹³, J.O. Thomas⁴², J.P. Thomas²¹, A.S. Thompson⁵⁷, P.D. Thompson²¹, L.A. Thomsen¹⁸³, E. Thomson¹³⁷, E.J. Thorpe⁹², R.E. Ticse Torres⁵³, V.O. Tikhomirov^{110,ap}, Yu.A. Tikhonov^{121b,121a}, S. Timoshenko¹¹¹, P. Tipton¹⁸³, S. Tisserant¹⁰¹, K. Todome^{23b,23a}, S. Todorova-Nova⁵, S. Todt⁴⁸, J. Tojo⁸⁷, S. Tokár^{28a}, K. Tokushuku⁸¹, E. Tolley¹²⁶, K.G. Tomiwa^{33d}, M. Tomoto¹¹⁶, L. Tompkins^{153,q}, B. Tong⁵⁹, P. Tornambe¹⁰², E. Torrence¹³¹, H. Torres⁴⁸, E. Torró Pastor¹⁴⁸, C. Tosciri¹³⁵, J. Toth^{101,ad}, D.R. Tovey¹⁴⁹, A. Traet¹⁷, C.J. Treado¹²⁴, T. Trefzger¹⁷⁷, F. Tresoldi¹⁵⁶, A. Tricoli²⁹, I.M. Trigger^{168a},

S. Trincas-Duvoid¹³⁶, W. Trischuk¹⁶⁷, B. Trocmé⁵⁸, A. Trofymov¹⁴⁵, C. Troncon^{68a}, M. Trovatelli¹⁷⁶,
 F. Trovato¹⁵⁶, L. Truong^{33b}, M. Trzebinski⁸⁴, A. Trzupek⁸⁴, F. Tsai⁴⁶, J.C.-L. Tseng¹³⁵, P.V. Tsiarashka^{107,aj},
 A. Tsirigotis¹⁶², V. Tsiskaridze¹⁵⁵, E.G. Tskhadadze^{159a}, M. Tsopoulou¹⁶², I.I. Tsukerman¹²³, V. Tsulaia¹⁸,
 S. Tsuno⁸¹, D. Tsybychev¹⁵⁵, Y. Tu^{63b}, A. Tudorache^{27b}, V. Tudorache^{27b}, T.T. Tulbure^{27a}, A.N. Tuna⁵⁹,
 S. Turchikhin⁷⁹, D. Turgeman¹⁸⁰, I. Turk Cakir^{4b,w}, R.J. Turner²¹, R.T. Turra^{68a}, P.M. Tuts³⁹,
 S. Tzamarias¹⁶², E. Tzovara⁹⁹, G. Ucchielli⁴⁷, K. Uchida¹⁶³, I. Ueda⁸¹, M. Ughetto^{45a,45b}, F. Ukegawa¹⁶⁹,
 G. Unal³⁶, A. Undrus²⁹, G. Unel¹⁷¹, F.C. Ungaro¹⁰⁴, Y. Unno⁸¹, K. Uno¹⁶³, J. Urban^{28b}, P. Urquijo¹⁰⁴,
 G. Usai⁸, Z. Uysal^{12d}, V. Vacek¹⁴², B. Vachon¹⁰³, K.O.H. Vadla¹³⁴, A. Vaidya⁹⁴, C. Valderanis¹¹³,
 E. Valdes Santurio^{45a,45b}, M. Valente⁵⁴, S. Valentinetti^{23b,23a}, A. Valero¹⁷⁴, L. Valéry⁴⁶, R.A. Vallance²¹,
 A. Vallier³⁶, J.A. Valls Ferrer¹⁷⁴, T.R. Van Daalen¹⁴, P. Van Gemmeren⁶, I. Van Vulpen¹¹⁹,
 M. Vanadia^{73a,73b}, W. Vandelli³⁶, E.R. Vandewall¹²⁹, A. Vaniachine¹⁶⁶, D. Vannicola^{72a,72b}, R. Vari^{72a},
 E.W. Varnes⁷, C. Varni^{55b,55a}, T. Varol¹⁵⁸, D. Varouchas¹³², K.E. Varvell¹⁵⁷, M.E. Vasile^{27b},
 G.A. Vasquez¹⁷⁶, J.G. Vasquez¹⁸³, F. Vazeille³⁸, D. Vazquez Furelos¹⁴, T. Vazquez Schroeder³⁶,
 J. Veatch⁵³, V. Vecchio^{74a,74b}, M.J. Veen¹¹⁹, L.M. Veloce¹⁶⁷, F. Veloso^{140a,140c}, S. Veneziano^{72a},
 A. Ventura^{67a,67b}, N. Venturi³⁶, A. Verbytskyi¹¹⁴, V. Vercesi^{70a}, M. Verducci^{71a,71b},
 C.M. Vergel Infante⁷⁸, C. Vergis²⁴, W. Verkerke¹¹⁹, A.T. Vermeulen¹¹⁹, J.C. Vermeulen¹¹⁹,
 M.C. Vetterli^{152,ax}, N. Viaux Maira^{147c}, M. Vicente Barreto Pinto⁵⁴, T. Vickey¹⁴⁹, O.E. Vickey Boeriu¹⁴⁹,
 G.H.A. Viehhauser¹³⁵, L. Vigani^{61b}, M. Villa^{23b,23a}, M. Villaplana Perez^{68a,68b}, E. Vilucchi⁵¹,
 M.G. Vinciter³⁴, G.S. Virdee²¹, A. Vishwakarma⁴⁶, C. Vittori^{23b,23a}, I. Vivarelli¹⁵⁶, M. Vogel¹⁸²,
 P. Vokac¹⁴², S.E. von Buddenbrock^{33d}, E. Von Toerne²⁴, V. Vorobel¹⁴³, K. Vorobev¹¹¹, M. Vos¹⁷⁴,
 J.H. Vosseveld⁹⁰, M. Vozak¹⁰⁰, N. Vranjes¹⁶, M. Vranjes Milosavljevic¹⁶, V. Vrba¹⁴², M. Vreeswijk¹¹⁹,
 R. Vuillermet³⁶, I. Vukotic³⁷, P. Wagner²⁴, W. Wagner¹⁸², J. Wagner-Kuhr¹¹³, S. Wahdan¹⁸²,
 H. Wahlberg⁸⁸, V.M. Walbrecht¹¹⁴, J. Walder⁸⁹, R. Walker¹¹³, S.D. Walker⁹³, W. Walkowiak¹⁵¹,
 V. Wallangen^{45a,45b}, A.M. Wang⁵⁹, C. Wang^{60c}, C. Wang^{60b}, F. Wang¹⁸¹, H. Wang¹⁸, H. Wang³,
 J. Wang^{63a}, J. Wang¹⁵⁷, J. Wang^{61b}, P. Wang⁴², Q. Wang¹²⁸, R.-J. Wang⁹⁹, R. Wang^{60a}, R. Wang⁶,
 S.M. Wang¹⁵⁸, W.T. Wang^{60a}, W. Wang^{15c,af}, W.X. Wang^{60a,af}, Y. Wang^{60a,am}, Z. Wang^{60c},
 C. Wanotayaroj⁴⁶, A. Warburton¹⁰³, C.P. Ward³², D.R. Wardrope⁹⁴, N. Warrack⁵⁷, A. Washbrook⁵⁰,
 A.T. Watson²¹, M.F. Watson²¹, G. Watts¹⁴⁸, B.M. Waugh⁹⁴, A.F. Webb¹¹, S. Webb⁹⁹, C. Weber¹⁸³,
 M.S. Weber²⁰, S.A. Weber³⁴, S.M. Weber^{61a}, A.R. Weidberg¹³⁵, J. Weingarten⁴⁷, M. Weirich⁹⁹,
 C. Weiser⁵², P.S. Wells³⁶, T. Wenaus²⁹, T. Wengler³⁶, S. Wenig³⁶, N. Wormes²⁴, M.D. Werner⁷⁸,
 M. Wessels^{61a}, T.D. Weston²⁰, K. Whalen¹³¹, N.L. Whallon¹⁴⁸, A.M. Wharton⁸⁹, A.S. White¹⁰⁵,
 A. White⁸, M.J. White¹, D. Whiteson¹⁷¹, B.W. Whitmore⁸⁹, W. Wiedenmann¹⁸¹, M. Wielers¹⁴⁴,
 N. Wieseotte⁹⁹, C. Wiglesworth⁴⁰, L.A.M. Wiik-Fuchs⁵², F. Wilk¹⁰⁰, H.G. Wilkens³⁶, L.J. Wilkins⁹³,
 H.H. Williams¹³⁷, S. Williams³², C. Willis¹⁰⁶, S. Willocq¹⁰², J.A. Wilson²¹, I. Wingerter-Seez⁵,
 E. Winkels¹⁵⁶, F. Winklmeier¹³¹, O.J. Winston¹⁵⁶, B.T. Winter⁵², M. Wittgen¹⁵³, M. Wobisch⁹⁵,
 A. Wolf⁹⁹, T.M.H. Wolf¹¹⁹, R. Wolff¹⁰¹, R.W. Wölker¹³⁵, J. Wollrath⁵², M.W. Wolter⁸⁴,
 H. Wolters^{140a,140c}, V.W.S. Wong¹⁷⁵, N.L. Woods¹⁴⁶, S.D. Worm²¹, B.K. Wosiek⁸⁴, K.W. Woźniak⁸⁴,
 K. Wraight⁵⁷, S.L. Wu¹⁸¹, X. Wu⁵⁴, Y. Wu^{60a}, T.R. Wyatt¹⁰⁰, B.M. Wynne⁵⁰, S. Xella⁴⁰, Z. Xi¹⁰⁵,
 L. Xia¹⁷⁸, X. Xiao¹⁰⁵, I. Xiotidis¹⁵⁶, D. Xu^{15a}, H. Xu^{60a,c}, L. Xu²⁹, T. Xu¹⁴⁵, W. Xu¹⁰⁵, Z. Xu^{60b}, Z. Xu¹⁵³,
 B. Yabsley¹⁵⁷, S. Yacoob^{33a}, K. Yajima¹³³, D.P. Yallup⁹⁴, D. Yamaguchi¹⁶⁵, Y. Yamaguchi¹⁶⁵,
 A. Yamamoto⁸¹, M. Yamatani¹⁶³, T. Yamazaki¹⁶³, Y. Yamazaki⁸², Z. Yan²⁵, H.J. Yang^{60c,60d}, H.T. Yang¹⁸,
 S. Yang⁷⁷, X. Yang^{60b,58}, Y. Yang¹⁶³, W.-M. Yao¹⁸, Y.C. Yap⁴⁶, Y. Yasu⁸¹, E. Yatsenko^{60c,60d}, J. Ye⁴²,
 S. Ye²⁹, I. Yeletsikh⁷⁹, M.R. Yexley⁸⁹, E. Yigitbasi²⁵, K. Yorita¹⁷⁹, K. Yoshihara¹³⁷, C.J.S. Young³⁶,
 C. Young¹⁵³, J. Yu⁷⁸, R. Yuan^{60b,i}, X. Yue^{61a}, S.P.Y. Yuen²⁴, M. Zaazoua^{35e}, B. Zabinski⁸⁴, G. Zacharis¹⁰,
 E. Zaffaroni⁵⁴, J. Zahreddine¹³⁶, A.M. Zaitsev^{122,ao}, T. Zakareishvili^{159b}, N. Zakharchuk³⁴, S. Zambito⁵⁹,
 D. Zanzi³⁶, D.R. Zaripovas⁵⁷, S.V. Zeiřner⁴⁷, C. Zeitnitz¹⁸², G. Zemaityte¹³⁵, J.C. Zeng¹⁷³, O. Zenin¹²²,
 T. Ženiř^{28a}, D. Zerwas¹³², M. Zgubić¹³⁵, B. Zhang^{15c}, D.F. Zhang^{15b}, G. Zhang^{15b}, H. Zhang^{15c},
 J. Zhang⁶, L. Zhang^{15c}, L. Zhang^{60a}, M. Zhang¹⁷³, R. Zhang²⁴, X. Zhang^{60b}, Y. Zhang^{15a,15d}, Z. Zhang^{63a},
 Z. Zhang¹³², P. Zhao⁴⁹, Y. Zhao^{60b}, Z. Zhao^{60a}, A. Zhemchugov⁷⁹, Z. Zheng¹⁰⁵, D. Zhong¹⁷³, B. Zhou¹⁰⁵,
 C. Zhou¹⁸¹, M.S. Zhou^{15a,15d}, M. Zhou¹⁵⁵, N. Zhou^{60c}, Y. Zhou⁷, C.G. Zhu^{60b}, C. Zhu^{15a,15d}, H.L. Zhu^{60a},
 H. Zhu^{15a}, J. Zhu¹⁰⁵, Y. Zhu^{60a}, X. Zhuang^{15a}, K. Zhukov¹¹⁰, V. Zhulanov^{121b,121a}, D. Zieminska⁶⁵,

N.I. Zimine⁷⁹, S. Zimmermann⁵², Z. Zinonos¹¹⁴, M. Ziolkowski¹⁵¹, L. Živković¹⁶, G. Zobernig¹⁸¹,
A. Zoccoli^{23b,23a}, K. Zoch⁵³, T.G. Zorbas¹⁴⁹, R. Zou³⁷, L. Zwalinski³⁶

- ¹ Department of Physics, University of Adelaide, Adelaide, Australia
- ² Physics Department, SUNY Albany, Albany, NY, United States of America
- ³ Department of Physics, University of Alberta, Edmonton, AB, Canada
- ⁴ (a) Department of Physics, Ankara University, Ankara; (b) Istanbul Aydin University, Istanbul; (c) Division of Physics, TOBB University of Economics and Technology, Ankara, Turkey
- ⁵ LAPP, Université Grenoble Alpes, Université Savoie Mont Blanc, CNRS/IN2P3, Annecy, France
- ⁶ High Energy Physics Division, Argonne National Laboratory, Argonne, IL, United States of America
- ⁷ Department of Physics, University of Arizona, Tucson, AZ, United States of America
- ⁸ Department of Physics, University of Texas at Arlington, Arlington, TX, United States of America
- ⁹ Physics Department, National and Kapodistrian University of Athens, Athens, Greece
- ¹⁰ Physics Department, National Technical University of Athens, Zografou, Greece
- ¹¹ Department of Physics, University of Texas at Austin, Austin, TX, United States of America
- ¹² (a) Bahcesehir University, Faculty of Engineering and Natural Sciences, Istanbul; (b) Istanbul Bilgi University, Faculty of Engineering and Natural Sciences, Istanbul; (c) Department of Physics, Bogazici University, Istanbul; (d) Department of Physics Engineering, Gaziantep University, Gaziantep, Turkey
- ¹³ Institute of Physics, Azerbaijan Academy of Sciences, Baku, Azerbaijan
- ¹⁴ Institut de Física d'Altes Energies (IFAE), Barcelona Institute of Science and Technology, Barcelona, Spain
- ¹⁵ (a) Institute of High Energy Physics, Chinese Academy of Sciences, Beijing; (b) Physics Department, Tsinghua University, Beijing; (c) Department of Physics, Nanjing University, Nanjing;
- ¹⁶ University of Chinese Academy of Science (UCAS), Beijing, China
- ¹⁷ Institute of Physics, University of Belgrade, Belgrade, Serbia
- ¹⁸ Department for Physics and Technology, University of Bergen, Bergen, Norway
- ¹⁹ Physics Division, Lawrence Berkeley National Laboratory and University of California, Berkeley, CA, United States of America
- ²⁰ Institut für Physik, Humboldt Universität zu Berlin, Berlin, Germany
- ²¹ Albert Einstein Center for Fundamental Physics and Laboratory for High Energy Physics, University of Bern, Bern, Switzerland
- ²² School of Physics and Astronomy, University of Birmingham, Birmingham, United Kingdom
- ²³ Facultad de Ciencias y Centro de Investigaciones, Universidad Antonio Nariño, Bogotá, Colombia
- ²⁴ (a) INFN Bologna and Università di Bologna, Dipartimento di Fisica; (b) INFN Sezione di Bologna, Italy
- ²⁵ Physikalisches Institut, Universität Bonn, Bonn, Germany
- ²⁶ Department of Physics, Boston University, Boston, MA, United States of America
- ²⁷ (a) Transilvania University of Brasov, Brasov; (b) Horia Hulubei National Institute of Physics and Nuclear Engineering, Bucharest; (c) Department of Physics, Alexandru Ioan Cuza University of Iasi, Iasi; (d) National Institute for Research and Development of Isotopic and Molecular Technologies, Physics Department, Cluj-Napoca; (e) University Politehnica Bucharest, Bucharest; (f) West University in Timisoara, Timisoara, Romania
- ²⁸ (a) Faculty of Mathematics, Physics and Informatics, Comenius University, Bratislava; (b) Department of Subnuclear Physics, Institute of Experimental Physics of the Slovak Academy of Sciences, Kosice, Slovak Republic
- ²⁹ Physics Department, Brookhaven National Laboratory, Upton, NY, United States of America
- ³⁰ Departamento de Física, Universidad de Buenos Aires, Buenos Aires, Argentina
- ³¹ California State University, CA, United States of America
- ³² Cavendish Laboratory, University of Cambridge, Cambridge, United Kingdom
- ³³ (a) Department of Physics, University of Cape Town, Cape Town; (b) Department of Mechanical Engineering Science, University of Johannesburg, Johannesburg; (c) Pretoria; (d) School of Physics, University of the Witwatersrand, Johannesburg, South Africa
- ³⁴ Department of Physics, Carleton University, Ottawa, ON, Canada
- ³⁵ (a) Faculté des Sciences Ain Chock, Réseau Universitaire de Physique des Hautes Energies – Université Hassan II, Casablanca; (b) Faculté des Sciences, Université Ibn-Tofail, Kénitra;
- ³⁶ (c) Faculté des Sciences Semlalia, Université Cadi Ayyad, LPHEA, Marrakech; (d) Faculté des Sciences, Université Mohamed Premier and LPTPM, Oujda; (e) Faculté des sciences, Université Mohammed V, Rabat, Morocco
- ³⁷ CERN, Geneva, Switzerland
- ³⁸ Enrico Fermi Institute, University of Chicago, Chicago, IL, United States of America
- ³⁹ LPC, Université Clermont Auvergne, CNRS/IN2P3, Clermont-Ferrand, France
- ⁴⁰ Nevis Laboratory, Columbia University, Irvington, NY, United States of America
- ⁴¹ Niels Bohr Institute, University of Copenhagen, Copenhagen, Denmark
- ⁴² (a) Dipartimento di Fisica, Università della Calabria, Rende; (b) INFN Gruppo Collegato di Cosenza, Laboratori Nazionali di Frascati, Italy
- ⁴³ Physics Department, Southern Methodist University, Dallas, TX, United States of America
- ⁴⁴ Physics Department, University of Texas at Dallas, Richardson, TX, United States of America
- ⁴⁵ National Centre for Scientific Research "Demokritos", Agia Paraskevi, Greece
- ⁴⁶ (a) Department of Physics, Stockholm University; (b) Oskar Klein Centre, Stockholm, Sweden
- ⁴⁷ Deutsches Elektronen-Synchrotron DESY, Hamburg and Zeuthen, Germany
- ⁴⁸ Lehrstuhl für Experimentelle Physik IV, Technische Universität Dortmund, Dortmund, Germany
- ⁴⁹ Institut für Kern- und Teilchenphysik, Technische Universität Dresden, Dresden, Germany
- ⁵⁰ Department of Physics, Duke University, Durham, NC, United States of America
- ⁵¹ SUPA – School of Physics and Astronomy, University of Edinburgh, Edinburgh, United Kingdom
- ⁵² INFN e Laboratori Nazionali di Frascati, Frascati, Italy
- ⁵³ Physikalisches Institut, Albert-Ludwigs-Universität Freiburg, Freiburg, Germany
- ⁵⁴ II. Physikalisches Institut, Georg-August-Universität Göttingen, Göttingen, Germany
- ⁵⁵ Département de Physique Nucléaire et Corpusculaire, Université de Genève, Genève, Switzerland
- ⁵⁶ (a) Dipartimento di Fisica, Università di Genova, Genova; (b) INFN Sezione di Genova, Italy
- ⁵⁷ II. Physikalisches Institut, Justus-Liebig-Universität Giessen, Giessen, Germany
- ⁵⁸ SUPA – School of Physics and Astronomy, University of Glasgow, Glasgow, United Kingdom
- ⁵⁹ LPSC, Université Grenoble Alpes, CNRS/IN2P3, Grenoble INP, Grenoble, France
- ⁶⁰ Laboratory for Particle Physics and Cosmology, Harvard University, Cambridge, MA, United States of America
- ⁶¹ (a) Department of Modern Physics and State Key Laboratory of Particle Detection and Electronics, University of Science and Technology of China, Hefei; (b) Institute of Frontier and Interdisciplinary Science and Key Laboratory of Particle Physics and Particle Irradiation (MOE), Shandong University, Qingdao; (c) School of Physics and Astronomy, Shanghai Jiao Tong University, KLPPAC-MOE, SKLPPC, Shanghai; (d) Tsung-Dao Lee Institute, Shanghai, China
- ⁶² (a) Kirchhoff-Institut für Physik, Ruprecht-Karls-Universität Heidelberg, Heidelberg; (b) Physikalisches Institut, Ruprecht-Karls-Universität Heidelberg, Heidelberg, Germany
- ⁶³ Faculty of Applied Information Science, Hiroshima Institute of Technology, Hiroshima, Japan
- ⁶⁴ (a) Department of Physics, Chinese University of Hong Kong, Shatin, N.T., Hong Kong; (b) Department of Physics, University of Hong Kong, Hong Kong; (c) Department of Physics and Institute for Advanced Study, Hong Kong University of Science and Technology, Clear Water Bay, Kowloon, Hong Kong, China
- ⁶⁵ Department of Physics, National Tsing Hua University, Hsinchu, Taiwan

- ⁶⁵ Department of Physics, Indiana University, Bloomington, IN, United States of America
- ⁶⁶ ^(a) INFN Gruppo Collegato di Udine, Sezione di Trieste, Udine; ^(b) ICTP, Trieste; ^(c) Dipartimento Politecnico di Ingegneria e Architettura, Università di Udine, Udine, Italy
- ⁶⁷ ^(a) INFN Sezione di Lecce; ^(b) Dipartimento di Matematica e Fisica, Università del Salento, Lecce, Italy
- ⁶⁸ ^(a) INFN Sezione di Milano; ^(b) Dipartimento di Fisica, Università di Milano, Milano, Italy
- ⁶⁹ ^(a) INFN Sezione di Napoli; ^(b) Dipartimento di Fisica, Università di Napoli, Napoli, Italy
- ⁷⁰ ^(a) INFN Sezione di Pavia; ^(b) Dipartimento di Fisica, Università di Pavia, Pavia, Italy
- ⁷¹ ^(a) INFN Sezione di Pisa; ^(b) Dipartimento di Fisica E. Fermi, Università di Pisa, Pisa, Italy
- ⁷² ^(a) INFN Sezione di Roma; ^(b) Dipartimento di Fisica, Sapienza Università di Roma, Roma, Italy
- ⁷³ ^(a) INFN Sezione di Roma Tor Vergata; ^(b) Dipartimento di Fisica, Università di Roma Tor Vergata, Roma, Italy
- ⁷⁴ ^(a) INFN Sezione di Roma Tre; ^(b) Dipartimento di Matematica e Fisica, Università Roma Tre, Roma, Italy
- ⁷⁵ ^(a) INFN-TIFPA; ^(b) Università degli Studi di Trento, Trento, Italy
- ⁷⁶ Institut für Astro- und Teilchenphysik, Leopold-Franzens-Universität, Innsbruck, Austria
- ⁷⁷ University of Iowa, Iowa City, IA, United States of America
- ⁷⁸ Department of Physics and Astronomy, Iowa State University, Ames, IA, United States of America
- ⁷⁹ Joint Institute for Nuclear Research, Dubna, Russia
- ⁸⁰ ^(a) Departamento de Engenharia Elétrica, Universidade Federal de Juiz de Fora (UFJF), Juiz de Fora; ^(b) Universidade Federal do Rio De Janeiro COPPE/EE/IF, Rio de Janeiro; ^(c) Universidade Federal de São João del Rei (UFSJ), São João del Rei; ^(d) Instituto de Física, Universidade de São Paulo, São Paulo, Brazil
- ⁸¹ KEK, High Energy Accelerator Research Organization, Tsukuba, Japan
- ⁸² Graduate School of Science, Kobe University, Kobe, Japan
- ⁸³ ^(a) AGH University of Science and Technology, Faculty of Physics and Applied Computer Science, Krakow; ^(b) Marian Smoluchowski Institute of Physics, Jagiellonian University, Krakow, Poland
- ⁸⁴ Institute of Nuclear Physics Polish Academy of Sciences, Krakow, Poland
- ⁸⁵ Faculty of Science, Kyoto University, Kyoto, Japan
- ⁸⁶ Kyoto University of Education, Kyoto, Japan
- ⁸⁷ Research Center for Advanced Particle Physics and Department of Physics, Kyushu University, Fukuoka, Japan
- ⁸⁸ Instituto de Física La Plata, Universidad Nacional de La Plata and CONICET, La Plata, Argentina
- ⁸⁹ Physics Department, Lancaster University, Lancaster, United Kingdom
- ⁹⁰ Oliver Lodge Laboratory, University of Liverpool, Liverpool, United Kingdom
- ⁹¹ Department of Experimental Particle Physics, Jožef Stefan Institute and Department of Physics, University of Ljubljana, Ljubljana, Slovenia
- ⁹² School of Physics and Astronomy, Queen Mary University of London, London, United Kingdom
- ⁹³ Department of Physics, Royal Holloway University of London, Egham, United Kingdom
- ⁹⁴ Department of Physics and Astronomy, University College London, London, United Kingdom
- ⁹⁵ Louisiana Tech University, Ruston, LA, United States of America
- ⁹⁶ Fysiska institutionen, Lunds universitet, Lund, Sweden
- ⁹⁷ Centre de Calcul de l'Institut National de Physique Nucléaire et de Physique des Particules (IN2P3), Villeurbanne, France
- ⁹⁸ Departamento de Física Teórica C-15 and CIAFF, Universidad Autónoma de Madrid, Madrid, Spain
- ⁹⁹ Institut für Physik, Universität Mainz, Mainz, Germany
- ¹⁰⁰ School of Physics and Astronomy, University of Manchester, Manchester, United Kingdom
- ¹⁰¹ CPPM, Aix-Marseille Université, CNRS/IN2P3, Marseille, France
- ¹⁰² Department of Physics, University of Massachusetts, Amherst, MA, United States of America
- ¹⁰³ Department of Physics, McGill University, Montreal, QC, Canada
- ¹⁰⁴ School of Physics, University of Melbourne, Victoria, Australia
- ¹⁰⁵ Department of Physics, University of Michigan, Ann Arbor, MI, United States of America
- ¹⁰⁶ Department of Physics and Astronomy, Michigan State University, East Lansing, MI, United States of America
- ¹⁰⁷ B.I. Stepanov Institute of Physics, National Academy of Sciences of Belarus, Minsk, Belarus
- ¹⁰⁸ Research Institute for Nuclear Problems of Byelorussian State University, Minsk, Belarus
- ¹⁰⁹ Group of Particle Physics, University of Montreal, Montreal, QC, Canada
- ¹¹⁰ P.N. Lebedev Physical Institute of the Russian Academy of Sciences, Moscow, Russia
- ¹¹¹ National Research Nuclear University MEPhI, Moscow, Russia
- ¹¹² D.V. Skobeltsyn Institute of Nuclear Physics, M.V. Lomonosov Moscow State University, Moscow, Russia
- ¹¹³ Fakultät für Physik, Ludwig-Maximilians-Universität München, München, Germany
- ¹¹⁴ Max-Planck-Institut für Physik (Werner-Heisenberg-Institut), München, Germany
- ¹¹⁵ Nagasaki Institute of Applied Science, Nagasaki, Japan
- ¹¹⁶ Graduate School of Science and Kobayashi-Maskawa Institute, Nagoya University, Nagoya, Japan
- ¹¹⁷ Department of Physics and Astronomy, University of New Mexico, Albuquerque, NM, United States of America
- ¹¹⁸ Institute for Mathematics, Astrophysics and Particle Physics, Radboud University Nijmegen/Nikhef, Nijmegen, Netherlands
- ¹¹⁹ Nikhef National Institute for Subatomic Physics and University of Amsterdam, Amsterdam, Netherlands
- ¹²⁰ Department of Physics, Northern Illinois University, DeKalb, IL, United States of America
- ¹²¹ ^(a) Budker Institute of Nuclear Physics and NSU, SB RAS, Novosibirsk; ^(b) Novosibirsk State University Novosibirsk, Russia
- ¹²² Institute for High Energy Physics of the National Research Centre Kurchatov Institute, Protvino, Russia
- ¹²³ Institute for Theoretical and Experimental Physics named by A.I. Alikhanov of National Research Centre "Kurchatov Institute", Moscow, Russia
- ¹²⁴ Department of Physics, New York University, New York, NY, United States of America
- ¹²⁵ Ochanomizu University, Otsuka, Bunkyo-ku, Tokyo, Japan
- ¹²⁶ Ohio State University, Columbus, OH, United States of America
- ¹²⁷ Faculty of Science, Okayama University, Okayama, Japan
- ¹²⁸ Homer L. Dodge Department of Physics and Astronomy, University of Oklahoma, Norman, OK, United States of America
- ¹²⁹ Department of Physics, Oklahoma State University, Stillwater, OK, United States of America
- ¹³⁰ Palacký University, RPTM, Joint Laboratory of Optics, Olomouc, Czech Republic
- ¹³¹ Center for High Energy Physics, University of Oregon, Eugene, OR, United States of America
- ¹³² LAL, Université Paris-Sud, CNRS/IN2P3, Université Paris-Saclay, Orsay, France
- ¹³³ Graduate School of Science, Osaka University, Osaka, Japan
- ¹³⁴ Department of Physics, University of Oslo, Oslo, Norway
- ¹³⁵ Department of Physics, Oxford University, Oxford, United Kingdom
- ¹³⁶ LPNHE, Sorbonne Université, Université de Paris, CNRS/IN2P3, Paris, France
- ¹³⁷ Department of Physics, University of Pennsylvania, Philadelphia, PA, United States of America
- ¹³⁸ Konstantinov Nuclear Physics Institute of National Research Centre "Kurchatov Institute", PNPI, St. Petersburg, Russia
- ¹³⁹ Department of Physics and Astronomy, University of Pittsburgh, Pittsburgh, PA, United States of America
- ¹⁴⁰ ^(a) Laboratório de Instrumentação e Física Experimental de Partículas – LIP, Lisboa; ^(b) Departamento de Física, Faculdade de Ciências, Universidade de Lisboa, Lisboa; ^(c) Departamento de Física, Universidade de Coimbra, Coimbra; ^(d) Centro de Física Nuclear da Universidade de Lisboa, Lisboa; ^(e) Departamento de Física, Universidade do Minho, Braga; ^(f) Departamento

- de Física Teórica y del Cosmos, Universidad de Granada, Granada (Spain); ^(g) Dep Física and CEFITEC of Faculdade de Ciências e Tecnologia, Universidade Nova de Lisboa, Caparica;
- ^(h) Instituto Superior Técnico, Universidade de Lisboa, Lisboa, Portugal
- ¹⁴¹ Institute of Physics of the Czech Academy of Sciences, Prague, Czech Republic
- ¹⁴² Czech Technical University in Prague, Prague, Czech Republic
- ¹⁴³ Charles University, Faculty of Mathematics and Physics, Prague, Czech Republic
- ¹⁴⁴ Particle Physics Department, Rutherford Appleton Laboratory, Didcot, United Kingdom
- ¹⁴⁵ IRFU, CEA, Université Paris-Saclay, Gif-sur-Yvette, France
- ¹⁴⁶ Santa Cruz Institute for Particle Physics, University of California Santa Cruz, Santa Cruz, CA, United States of America
- ¹⁴⁷ ^(a) Departamento de Física, Pontificia Universidad Católica de Chile, Santiago; ^(b) Universidad Andres Bello, Department of Physics, Santiago; ^(c) Departamento de Física, Universidad Técnica Federico Santa María, Valparaíso, Chile
- ¹⁴⁸ Department of Physics, University of Washington, Seattle, WA, United States of America
- ¹⁴⁹ Department of Physics and Astronomy, University of Sheffield, Sheffield, United Kingdom
- ¹⁵⁰ Department of Physics, Shinshu University, Nagano, Japan
- ¹⁵¹ Department Physik, Universität Siegen, Siegen, Germany
- ¹⁵² Department of Physics, Simon Fraser University, Burnaby, BC, Canada
- ¹⁵³ SLAC National Accelerator Laboratory, Stanford, CA, United States of America
- ¹⁵⁴ Physics Department, Royal Institute of Technology, Stockholm, Sweden
- ¹⁵⁵ Departments of Physics and Astronomy, Stony Brook University, Stony Brook, NY, United States of America
- ¹⁵⁶ Department of Physics and Astronomy, University of Sussex, Brighton, United Kingdom
- ¹⁵⁷ School of Physics, University of Sydney, Sydney, Australia
- ¹⁵⁸ Institute of Physics, Academia Sinica, Taipei, Taiwan
- ¹⁵⁹ ^(a) E. Andronikashvili Institute of Physics, Iv. Javakishvili Tbilisi State University, Tbilisi; ^(b) High Energy Physics Institute, Tbilisi State University, Tbilisi, Georgia
- ¹⁶⁰ Department of Physics, Technion, Israel Institute of Technology, Haifa, Israel
- ¹⁶¹ Raymond and Beverly Sackler School of Physics and Astronomy, Tel Aviv University, Tel Aviv, Israel
- ¹⁶² Department of Physics, Aristotle University of Thessaloniki, Thessaloniki, Greece
- ¹⁶³ International Center for Elementary Particle Physics and Department of Physics, University of Tokyo, Tokyo, Japan
- ¹⁶⁴ Graduate School of Science and Technology, Tokyo Metropolitan University, Tokyo, Japan
- ¹⁶⁵ Department of Physics, Tokyo Institute of Technology, Tokyo, Japan
- ¹⁶⁶ Tomsk State University, Tomsk, Russia
- ¹⁶⁷ Department of Physics, University of Toronto, Toronto, ON, Canada
- ¹⁶⁸ ^(a) TRIUMF, Vancouver, BC; ^(b) Department of Physics and Astronomy, York University, Toronto, ON, Canada
- ¹⁶⁹ Division of Physics and Tomonaga Center for the History of the Universe, Faculty of Pure and Applied Sciences, University of Tsukuba, Tsukuba, Japan
- ¹⁷⁰ Department of Physics and Astronomy, Tufts University, Medford, MA, United States of America
- ¹⁷¹ Department of Physics and Astronomy, University of California Irvine, Irvine, CA, United States of America
- ¹⁷² Department of Physics and Astronomy, University of Uppsala, Uppsala, Sweden
- ¹⁷³ Department of Physics, University of Illinois, Urbana, IL, United States of America
- ¹⁷⁴ Instituto de Física Corpuscular (IFIC), Centro Mixto Universidad de Valencia – CSIC, Valencia, Spain
- ¹⁷⁵ Department of Physics, University of British Columbia, Vancouver, BC, Canada
- ¹⁷⁶ Department of Physics and Astronomy, University of Victoria, Victoria, BC, Canada
- ¹⁷⁷ Fakultät für Physik und Astronomie, Julius-Maximilians-Universität Würzburg, Würzburg, Germany
- ¹⁷⁸ Department of Physics, University of Warwick, Coventry, United Kingdom
- ¹⁷⁹ Waseda University, Tokyo, Japan
- ¹⁸⁰ Department of Particle Physics, Weizmann Institute of Science, Rehovot, Israel
- ¹⁸¹ Department of Physics, University of Wisconsin, Madison, WI, United States of America
- ¹⁸² Fakultät für Mathematik und Naturwissenschaften, Fachgruppe Physik, Bergische Universität Wuppertal, Wuppertal, Germany
- ¹⁸³ Department of Physics, Yale University, New Haven, CT, United States of America
- ¹⁸⁴ Yerevan Physics Institute, Yerevan, Armenia

^a Also at Borough of Manhattan Community College, City University of New York, New York NY; United States of America.

^b Also at CERN, Geneva; Switzerland.

^c Also at CPPM, Aix-Marseille Université, CNRS/IN2P3, Marseille; France.

^d Also at Département de Physique Nucléaire et Corpusculaire, Université de Genève, Genève; Switzerland.

^e Also at Departament de Física de la Universitat Autònoma de Barcelona, Barcelona; Spain.

^f Also at Departamento de Física, Instituto Superior Técnico, Universidade de Lisboa, Lisboa; Portugal.

^g Also at Department of Applied Physics and Astronomy, University of Sharjah, Sharjah; United Arab Emirates.

^h Also at Department of Financial and Management Engineering, University of the Aegean, Chios; Greece.

ⁱ Also at Department of Physics and Astronomy, Michigan State University, East Lansing MI; United States of America.

^j Also at Department of Physics and Astronomy, University of Louisville, Louisville, KY; United States of America.

^k Also at Department of Physics, Ben Gurion University of the Negev, Beer Sheva; Israel.

^l Also at Department of Physics, California State University, East Bay; United States of America.

^m Also at Department of Physics, California State University, Fresno; United States of America.

ⁿ Also at Department of Physics, California State University, Sacramento; United States of America.

^o Also at Department of Physics, King's College London, London; United Kingdom.

^p Also at Department of Physics, St. Petersburg State Polytechnical University, St. Petersburg; Russia.

^q Also at Department of Physics, Stanford University, Stanford CA; United States of America.

^r Also at Department of Physics, University of Adelaide, Adelaide; Australia.

^s Also at Department of Physics, University of Fribourg, Fribourg; Switzerland.

^t Also at Department of Physics, University of Michigan, Ann Arbor MI; United States of America.

^u Also at Dipartimento di Matematica, Informatica e Fisica, Università di Udine, Udine; Italy.

^v Also at Faculty of Physics, M.V. Lomonosov Moscow State University, Moscow; Russia.

^w Also at Giresun University, Faculty of Engineering, Giresun; Turkey.

^x Also at Graduate School of Science, Osaka University, Osaka; Japan.

^y Also at Hellenic Open University, Patras; Greece.

^z Also at Institutio Catalana de Recerca i Estudis Avancats, ICREA, Barcelona; Spain.

^{aa} Also at Institut für Experimentalphysik, Universität Hamburg, Hamburg; Germany.

^{ab} Also at Institute for Mathematics, Astrophysics and Particle Physics, Radboud University Nijmegen/Nikhef, Nijmegen; Netherlands.

^{ac} Also at Institute for Nuclear Research and Nuclear Energy (INRNE) of the Bulgarian Academy of Sciences, Sofia; Bulgaria.

- ^{ad} Also at Institute for Particle and Nuclear Physics, Wigner Research Centre for Physics, Budapest; Hungary.
- ^{ae} Also at Institute of Particle Physics (IPP), Vancouver; Canada.
- ^{af} Also at Institute of Physics, Academia Sinica, Taipei; Taiwan.
- ^{ag} Also at Institute of Physics, Azerbaijan Academy of Sciences, Baku; Azerbaijan.
- ^{ah} Also at Institute of Theoretical Physics, Ilia State University, Tbilisi; Georgia.
- ^{ai} Also at Instituto de Fisica Teorica, IFT-UAM/CSIC, Madrid; Spain.
- ^{aj} Also at Joint Institute for Nuclear Research, Dubna; Russia.
- ^{ak} Also at LAL, Université Paris-Sud, CNRS/IN2P3, Université Paris-Saclay, Orsay; France.
- ^{al} Also at Louisiana Tech University, Ruston LA; United States of America.
- ^{am} Also at LPNHE, Sorbonne Université, Université de Paris, CNRS/IN2P3, Paris; France.
- ^{an} Also at Manhattan College, New York NY; United States of America.
- ^{ao} Also at Moscow Institute of Physics and Technology State University, Dolgoprudny; Russia.
- ^{ap} Also at National Research Nuclear University MEPhI, Moscow; Russia.
- ^{aq} Also at Physics Department, An-Najah National University, Nablus; Palestine.
- ^{ar} Also at Physics Dept, University of South Africa, Pretoria; South Africa.
- ^{as} Also at Physikalisches Institut, Albert-Ludwigs-Universität Freiburg, Freiburg; Germany.
- ^{at} Also at School of Physics, Sun Yat-sen University, Guangzhou; China.
- ^{au} Also at The City College of New York, New York NY; United States of America.
- ^{av} Also at The Collaborative Innovation Center of Quantum Matter (CICQM), Beijing; China.
- ^{aw} Also at Tomsk State University, Tomsk, and Moscow Institute of Physics and Technology State University, Dolgoprudny; Russia.
- ^{ax} Also at TRIUMF, Vancouver BC; Canada.
- ^{ay} Also at Università di Napoli Parthenope, Napoli; Italy.
- * Deceased.